Advances in Desiccant Wheels for Dehumidification, VOC Mitigation, and CO_2 Removal for Energy-Efficient IAQ Management

[1,§]Jubair A. Shamim, [1,§]Xiaoli Liu, [1]Easwaran Krishnan, [1]Kai Li, [1]M Murugan, [2]Huixin Jiang, [1]Poorandokht Ilani-Kashkouli, [1,*]Kashif Nawaz

[1]*Buildings and Transportation Science Division, Building Technologies Research and Integration Center (BTRIC), Oak Ridge National Laboratory, Oak Ridge, TN 37830, United States*

[2]*Chemical Sciences Division, Oak Ridge National Laboratory, Oak Ridge, TN 37830, United States*

[§]These authors have contributed equally.

*Corresponding author's email:

nawazk@ornl.gov

Abstract

Humidity control is pivotal to maintain occupant thermal comfort and suppress mold growth in indoor environments. Furthermore, poor indoor air quality (IAQ) due to the presence of volatile organic compounds (VOCs) and high concentrations (>1,000 ppm) of CO_2 can cause health issues and negatively affect cognitive performance. Therefore, providing high-quality indoor air has gained significant attention over the past decade. Conventional cooling coil and filter-based HVAC systems have limited capability to meet the augmented demand for occupant thermal comfort and high indoor air quality. Moreover, modern buildings are increasingly airtight to save energy, and increasing ventilation to mitigate VOC and CO_2 concentration is discouraged. Separate sensible and latent cooling technology using a rotary desiccant wheel presents a promising solution in this respect. Because of the development of desiccant materials with high water vapor, VOC, and CO_2 uptake, desiccant wheels can be used as an integrated technology option for IAQ management. To promote desiccant wheel use for energy-efficient management of IAQ in buildings, this article reviews recent advancements in using desiccant wheels for dehumidification, VOC mitigation, and CO_2 capture from outdoor air. Finally, the article presents the authors' perspective by summarizing the key research gaps in the field and discussing the future direction of research to address these gaps from two different aspects, namely, suitable adsorbent material development and desiccant wheel design.

Keywords: indoor air quality, desiccant wheel; dehumidification; volatile organic compounds; CO_2 capture.

1 Introduction

1.1 Context

Humidity control in indoor environments is crucial to ensure adequate thermal comfort and prevent sick building syndrome. 2020 ASHRAE handbook-HVAC Systems and Equipment[1] states that optimal indoor humidity is around 30%–60%. The energy consumption and emissions associated with humidity control are high but often overlooked. Humidity control with air conditioners is responsible for emitting 599 million tons of CO_2 annually [2]. Because of high needs for thermal comfort in built environments and highly efficient building envelope design, along with increasing ventilation demands, the energy consumption for latent load management is expected to surpass the energy consumption for sensible load management by 2050, and the humidity load fraction is projected to increase by 54%–67% [2]. To accommodate this additional latent load management demand, existing HVAC systems will need to be retrofitted and redesigned. Conventional air-conditioning system dehumidifies air below the dew point in a cooling coil, where the water vapor condenses from the humid air **(Figure 1a)**. As a result, the air must be reheated, leading to significant energy waste. On the contrary, a desiccant-based system dehumidifies air at relatively higher temperatures by adsorbing water vapor into a porous medium **(Figure 1b)**. Thus, it eliminates the need for deep cooling of air for dehumidification.

However, in a desiccant system, air temperature rises from the release of enthalpy of adsorption, and a simple evaporative cooler can be used to control the supply air temperature. By handling the humidity and temperature separately, solid desiccant-based systems provide a more energy-efficient means to ensure thermal comfort. Nevertheless, a major limitation of the desiccant-based system is that the adsorbent can be quickly saturated with water vapor, so frequent/continuous regeneration of the adsorbent is necessary, which reduces the overall system coefficient of performance (COP). The most common desiccant dehumidification system with a high technology readiness level (TRL 8–9) is a desiccant wheel (DW), which provides continuous adsorption and regeneration. The typical footprint of a DW is smaller than that of fixed-bed systems, as the DW does not require batch-mode operation [3].

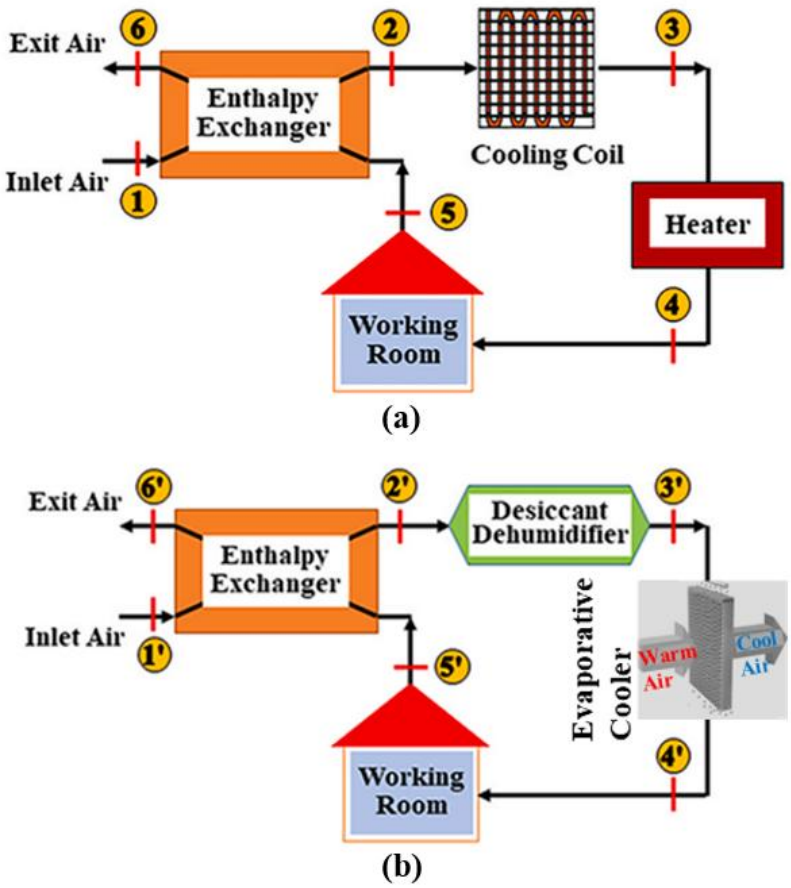

Figure 1. Illustration of air dehumidification process in conventional and desiccant-based system. (a) Schematic of a conventional cooling coil–based air-conditioning system that dehumidifies air below the dew point [4], and (b) Schematic of desiccant-based air-conditioning system that separates the separate sensible (temperature) and latent (moisture) load control and eliminates the necessity of cooling down the air below its dew point, and thus saves primary energy [4].

Along with maintaining appropriate humidity levels for thermal comfort, ensuring high indoor air quality (IAQ) is also important in office and educational settings, particularly by removing volatile organic compounds (VOCs) [5] and high-concentration CO_2 [6]. Poor IAQ often results in discomfort and sensory irritation, affect sleep quality, reduce productivity, and increase absenteeism [7, 8]. Prolonged exposure to VOCs can cause sick building syndrome and a range of health issues, including sensory irritations, respiratory diseases, and long-term toxic reactions [9]. Furthermore, moderate to elevated indoor CO_2 levels may adversely affect cognitive performance [10]. Therefore, indoor air must be free of VOCs, and the concentration of CO_2 should be below 1,000 ppm [11]. One way to maintain adequate IAQ levels is to increase the ventilation rate in the

indoor space. Studies have shown that ventilation rates below 10 Ls^{-1} per person were associated with one or more health issues, and increased ventilation up to 20 Ls^{-1} per person helped to abate sick building syndrome [11]. However, modern sustainable buildings are designed to be airtight to reduce energy consumption. Therefore, energy-efficient HVAC components must be developed to ensure proper IAQ at minimal energy consumption [12]. Moreover, in buildings alongside roads and in highly polluted and dusty areas, increased ventilation is not a viable solution. Consequently, use of portable air cleaners has been steadily growing in the past decade [13], which again leads to higher energy consumption and equipment cost. Designing an integrated indoor air supply system capable of maintaining thermal comfort by moisture removal, and improving indoor air quality by removing VOC content, and reducing CO_2 concentration, has the potential to save energy consumption for IAQ management in the buildings.

1.2 The Concept of Integrating DWs for Dehumidification, VOCs and CO_2 Capture

Existing literature report that along with moisture removal, DWs can be used in VOC mitigation [14] and direct air capture of CO_2 [15]. **Figure 2** depicts the concept diagram to employ three DWs in series in an integrated air supply unit to maintain thermal comfort and to improve IAQ (by removing VOCs and capturing CO_2) simultaneously. In this proposed arrangement, DW1, DW2 and DW3 will adsorb water vapor, VOC and CO_2, respectively from the supply air. Separate desiccant materials could be utilized in three DWs. Desiccants that exhibit preferential adsorption of water vapor over VOC and CO_2 should be used in DW1. Similarly, desiccant exhibited high VOC and CO_2 uptake should be used in DW2 and DW3 respectively. The moisture from the incoming supply air should be removed at first prior to VOC and CO2 removal (in other words; DW for moisture removal should be placed at first) since previous studies[16, 17] reported the evidence of reduced VOC and CO_2 uptake capacity by solid desiccants in the presence of water vapor. Furthermore, stability of newly derived desiccants such as MOFs can also be affected by the presence of water molecules. Following moisture removal, the rotary wheels dedicated for VOCs removal and then for CO_2 capture can be placed. Previous study on gaseous contaminant transfer in silica gel and molecular sieve wheels, conducted by Krishnan et al. [18] showed that the contaminants having high polarity and water solubility (e.g., ammonia, acetaldehyde, Xylene and Hexane) were adsorbed more readily than non-polar and non-reactive contaminants like

CO_2.The results of this study is shown in **Figure A1** in the appendix section. Hence, prior capturing CO_2, it is recommended to remove high polarity VOC contaminants from the airstream to improve the overall removal efficiency of the integrated system.

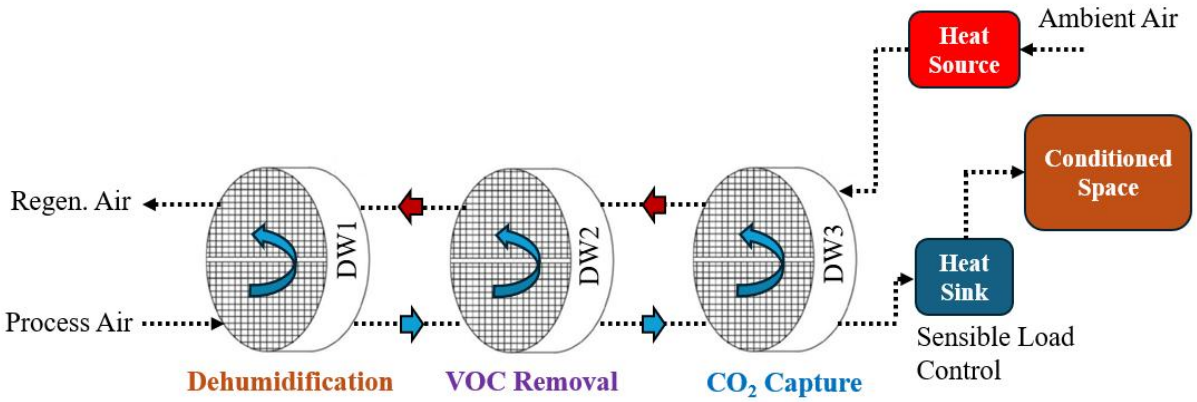

Figure 2. Concept diagram illustrating utilization of three DWs in an integrated system to maintain high IAQ. DW1, DW2 and DW3 are dedicated to moisture removal, VOC removal and CO_2 capture, respectively. Separate adsorbents tailored for high water vapor, VOC and CO2 uptake should be considered for each of the three DWs.

1.3 Previous Studies and Contribution of the Current Article

Previous reviews pertaining to DWs primarily focus on desiccant materials and dehumidification using various designs, including packed bed, fluidized bed, DW, desiccant-coated heat exchanger, and multilayer fixed-bed systems. For example, Shamim et al. [4] reviewed the state-of-the-art desiccant technologies suitable for hybrid air-conditioning in the context of net zero buildings. Asim et al. [19] reviewed the potential of silica- and carbon-based desiccant materials to attain higher system performance, particularly discussing their composition, microstructure, and preparation methods. Vivek et al. [20] and Venegas et al. [21] reviewed the advances in developing desiccant-coated heat exchangers, relevant materials, and manufacturing technology. Wu et al. [22] reviewed the influence of various substrate materials, such as glass and ceramic fiber based papers, and substrate shapes (e.g., sinusoidal air channels) on the dehumidification performance of both DW and desiccant coated heat exchangers.

Zaki et al. [23] reviewed and compared the performance of various technologies for sensible and latent cooling and concluded that vapor compression systems are effective for sensible loads, and desiccant systems are preferable for latent cooling. Jani et al. [24] and Rambhad et al. [25] also reviewed the progress in developing various solid desiccant materials and dehumidifiers and their system-level integration, particularly aimed at separate sensible and latent load control. Ge et al. [26] reviewed the progress made in desiccant wheel cooling system powered by various solar collectors, Tian et al. [27] reviewed the desiccant wheels coupled with heat pump system, Abd-Elhady et al. [28] reviewed various configurations used in solid desiccant dehumidification including desiccant wheel, packed and fluidized beds, Su et al. [29] reviewed the dehumidification technologies appropriate for industrial settings with low humidity environment.

From the survey of literature mentioned above, it is obvious that reviews solely focusing on DW in detail and discussing its potential beyond humidity control (i.e., for VOC and CO_2 removal) is not reported yet. This fact was further confirmed by conducting a literature search in web of science database using four different combinations of keywords. The outcome of the literature search is shown in **Figure 3**, where we can see that as of February 9, 2025, a total of 33 and 18 review articles are published for the keywords "Desiccant Wheel" and "Desiccant Wheel+ Dehumidification", respectively. However, no review articles are reported for the keywords "Desiccant Wheel+ VOC" and "Desiccant Wheel+ CO_2". Therefore, to address the identified research gap, this article presents an in-depth discussion on the state-of-the-art research achievements in using DWs in air dehumidification, VOC mitigation, and CO_2 capture with respect to IAQ management in the built environment.

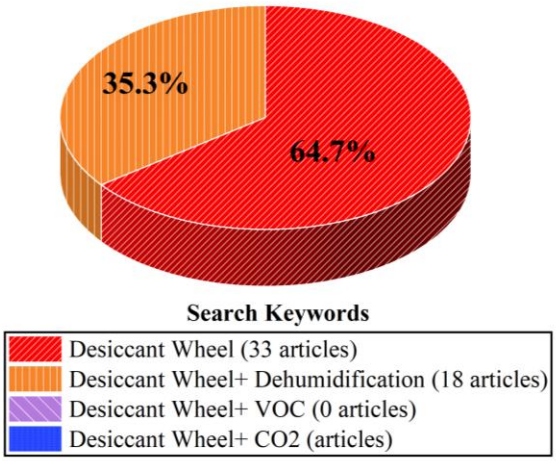

Figure 3. The outcome of literature search with four different keyword combinations in web of science database. 33 and 18 reviews have been published to date containing the keywords "desiccant wheel" and "desiccant wheel+ dehumidification", respectively in the article title. While no reviews are found with the keywords "desiccant wheel+VOC" and "desiccant wheel+CO_2".

1.4 Article Organization and Literature Search Method

The organization of the article is as follows: first, the article presents an overview of DWs for dehumidification in the built environment, progress in developing advanced materials, and designing advanced systems. Then, the next two sections present the progress made in the use of DWs in VOC and CO_2 removal. Finally, the research gaps from the perspectives of suitable desiccant material development and advanced DW design are presented, and future directions of research to address these gaps are discussed.

The literature search method of the current work employed a targeted keyword search strategy to identify relevant articles across three key areas: dehumidification, VOC removal, and CO_2 capture. The authors primarily utilized "Google Scholar" and "Web of Science" as the search engine. **Table A1** in the appendix section lists the most frequently used keyword for literature search. To be noted that these keywords were used either as a single word or as combinations of different words. The authors conducted the literature search from time to time over a long period from October 2022 to February 2025. In addition, several important journals in the field were identified and the literature search were also conducted in those journals' web page. Initially, the authors reviewed the titles and abstracts of the articles retrieved from these searches. Subsequently, the selection was narrowed down only to those articles found most relevant to each specific topic. A thorough examination of the shortlisted papers led to the final selection of 150 journal articles deemed appropriate and pertinent for inclusion in this review. For journal articles, only those written in English and published in reputed peer-reviewed journals were included. The primary objective of this review is to present advancements in the specified fields based on published literature from the past decade. However, some older foundational studies were also included, as they are essential for understanding the scientific concepts underlying current research.

2 Adsorption in Porous Media

2.1 Mechanisms

i) Interactive forces and binding energy: Gas adsorption in porous media can be divided into physisorption and chemisorption. Physisorption occurs when the gas molecules (adsorbate) are attached to the pore surface (adsorbent) due to the weak van der Waals forces. Since it is a weak and reversible intermolecular attraction, the binding energy between the adsorbate and adsorbent molecules are small, favoring low regeneration heat input to desorb the adsorbate molecules. Therefore, physisorption is the preferred mechanism when porous adsorbents are intended to be used for heat and moisture transfer applications. However, if the adsorbate molecules are highly polar in nature, electrostatic interaction between the adsorbate and adsorbent molecules may appear too, which will augment the binding energy and lead to increased heat input for regeneration. In chemisorption, the intermolecular forces involved lead to the formation of chemical bonds. Thus, the binding energy in chemisorption is considerably high, and hence chemisorption is not the preferred method for heat transformation related applications. Adsorption can also be categorized as thermal swing adsorption (TSA) and pressure swing adsorption (PSA). In TSA method, heat is used as input for regeneration, and enthalpy of gas adsorption is released due to the bond formation between the adsorbate and adsorbent molecules. In PSA method, adsorption takes place under high pressure environment and desorption of adsorbate molecules occurs when the pressure is released.

ii) Adsorption isotherms: Adsorption in porous media is characterized by the so-called adsorption isotherms, where the amount of gas adsorbed (in Y-axis) is plotted against the relative pressure of gas adsorption (in X-axis). In the case of water vapor, the relative pressure refers to the relative humidity. The measurement can be done either by using gravimetric or volumetric apparatus. The amount adsorbed is typically quantified as mass adsorbed per unit mass of adsorbent in the case of gravimetric measurement or volume adsorbed per unit mass of adsorbent in the case of volumetric measurement. The International Union of Pure Applied Chemistry (IUPAC) classifies the adsorption isotherms into five categories (i.e., Type-I to Type-V) based on the shapes of adsorption isotherm. Details on each of these categories are discusses in the review of Al-Ghouti and Da'ana [30]. Type-4 isotherm (S-shape) is the most preferred one for

dehumidification application. A good number of models are also proposed for different types of isotherms which are discussed in detail in the review of Majd et al. [31].

iii) Mass transport mechanism: In a typical traditional adsorbent such as silica gel, transport of water vapor from the pore entrance to the interior will take place in the following two steps: (i) transport from the bulk to the surface of the porous spheres (interparticle resistance) and (ii) transport inside the porous spheres (intraparticle resistance). A graphical illustration of these processes in a typical silica gel (M.S. Gel) in the glass tube of a volumetric setup is shown in **Figure 4a [32]**. The interparticle resistance is characterized by molecular diffusion, and the intraparticle resistance is characterized by surface diffusion and Knudsen diffusion (to be considered when the pore size is comparable or smaller than the mean free path of the gas molecules). Thus, the effective diffusivity should be determined for characterization of mass transport in porous media. Modeling of effective diffusivity in a silica gel packed bed and desiccant coated fin tube heat exchanger are presented in the study of Pesaran and Mills [33] and Li et al. [34], respectively.

Several other factors will also influence the transport phenomena within a porous substance, e.g., pore size distribution, porosity, specific surface area, and pore volume), topologies (i.e., connectivity and tortuosity), and pore chemistry (i.e., hydrophilic or hydrophobic) [35, 36]. Well-connected pores are desirable for better dehumidification performance. Furthermore, large interior surface area of pores and pore volume with less geometric barrier are beneficial for large adsorption capacity. Therefore, a combination of micropores (typical pore diameter $\leq$2 nm) and mesopores (typical pore diameter ranges between 2-50 nm) could potentially lead to high-efficient adsorption [37].

iv) Pore filling process: Regarding the pore filling process in traditional adsorbents with multiscale porous structure, the two well-known theories in the literature are multilayer adsorption proposed by Brunauer et al. (a.k.a. BET theory) and capillary condensation represented by the Kelvin equation [38]. In a typical adsorbent material with S-shape isotherm (IUPAC type-IV), adsorption begins with monolayer coverage where all adsorbed molecules directly interact with the surface layer. With increasing vapor pressure, multilayer adsorption occurs, forming a liquid

bridge with a concave meniscus in the middle region in the case of a cylindrical pore. This will initiate the capillary condensation with accelerated adsorption and completion of the pore-filling process. A graphical illustration of this pore-filling process in a cylindrical hydrophilic pore is shown in **Figure 4b** [39]**.** The onset of different pore-filling steps on a typical S-shape isotherm is illustrated in **Figure 4c** [40].

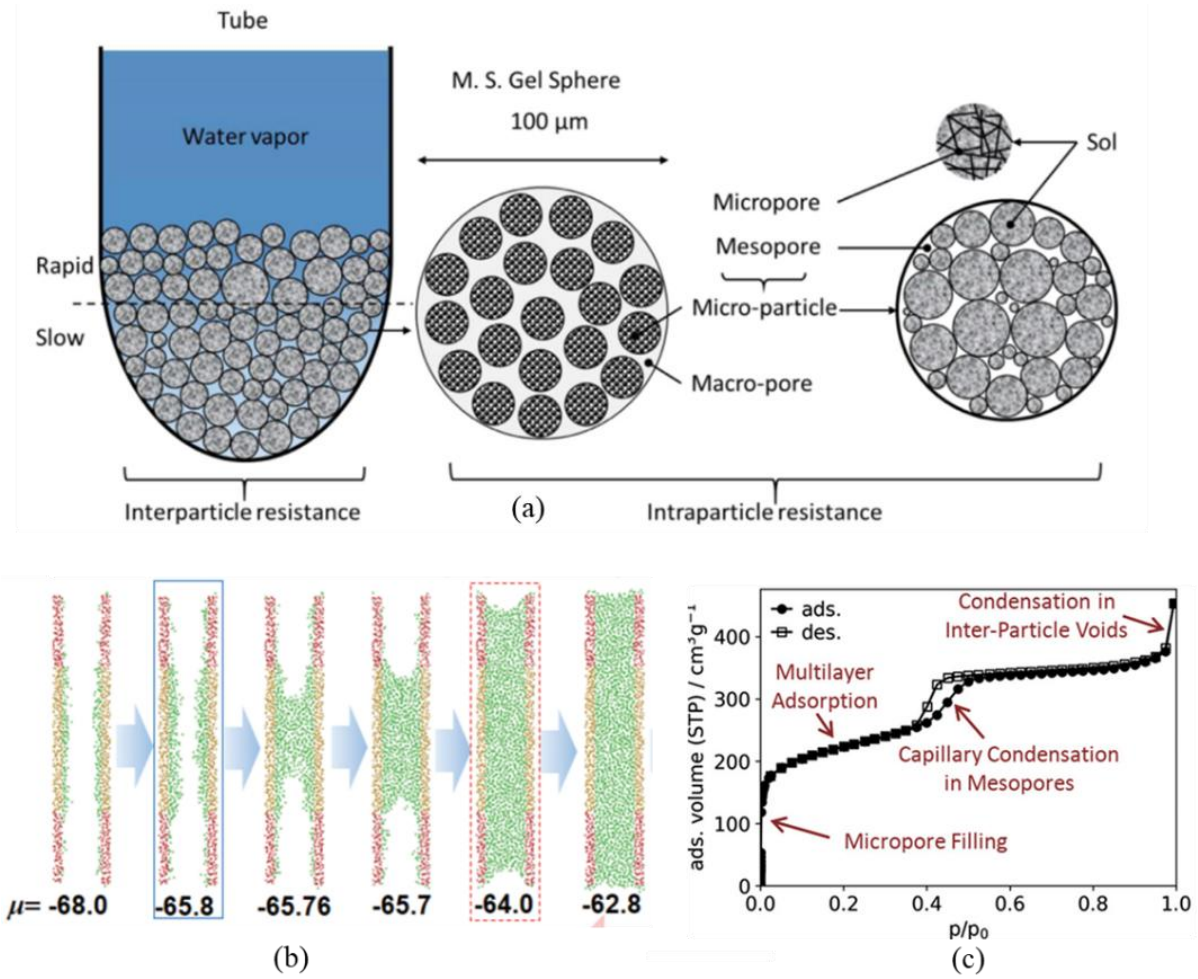

Figure 4. Adsorption mechanism in porous materials. (a) Illustration of interparticle and intraparticle mass transfer resistance in a typical silica gel (M.S. Gel) consisting of macro, meso, and micropores [32], (b) Illustration of pore filling process (multilayer adsorption and capillary condensation) in a cylindrical hydrophilic pore (µ represents chemical potential) [39], and (c) Graphical representation of the onset of different pore-filling steps on a typical S-shape (IUPAC Type-IV) isotherm [40].

3 DWs for Dehumidification

3.1 Working principle and configurations of DW

The schematic and operating principle of a DW intended for air dehumidification in the buildings is shown in **Figure 5**, which is similar to a counter-flow energy exchanger with state profiles (i.e., relative humidity [RH], temperature, and gas uptake). Process air flows through one side (approximately 1/2 to 3/4 of the area), while regeneration air flows through the remaining side (1/4 of the area). Water vapor is removed from the matrix area exposed to the process air side of the wheel as the wheel rotates, and at the same time, water vapor is released from the matrix area exposed to regeneration air. Further details on the operation of DW is reported in ref [41]. From the design viewpoint, two configurations of DW are feasible, namely, single-stage with internal cooling and interstage cooling, which are elaborated below.

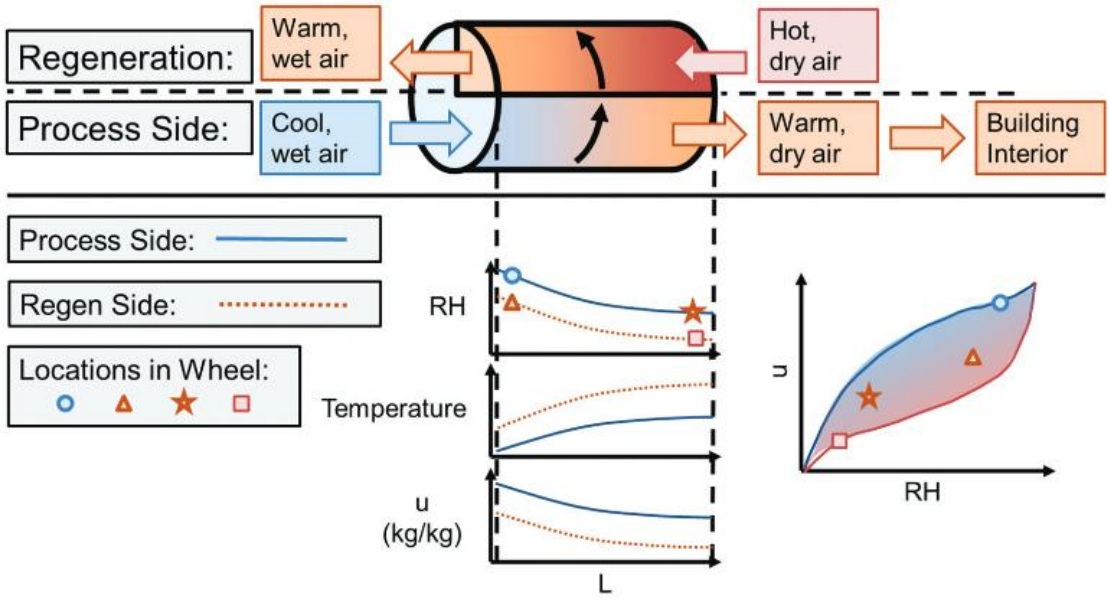

Figure 5. Schematic and working principles of the DW [41].

i) Single-stage with internal cooling

Conventional DWs comprise multiple channels coated with a desiccant through which both process air and regeneration air streams pass intermittently. Because of the exothermic nature of adsorption, the temperature of the desiccant and substrate increases when it adsorbs water vapor from process air, and this adiabatic dehumidification process limits the humification capacity of

the wheel [42, 43]. The limitation may be resolved by removing the enthalpy of adsorption to achieve the adsorption process semi-isothermal or isothermal. **Figure 6a** depicts the different dehumidification scenarios for a DW in a Mollier diagram [23]. Using a multilayer fixed-bed binder-free desiccant dehumidifier (MFBDD) [44-46], Shamim et al. [4] demonstrated that ideal isothermal dehumidification ($T_{\text{bed constant}}$ in **Figure 6b**) could enhance the mass of water vapor adsorbed (m_{ads}) in a desiccant bed by more than 100% for a 300 s adsorption time (**Figure 6c**) compared with the case when bed temperature increased ($T_{\text{bed variable}}$ **Figure 6b**) due to the release of the enthalpy of adsorption.

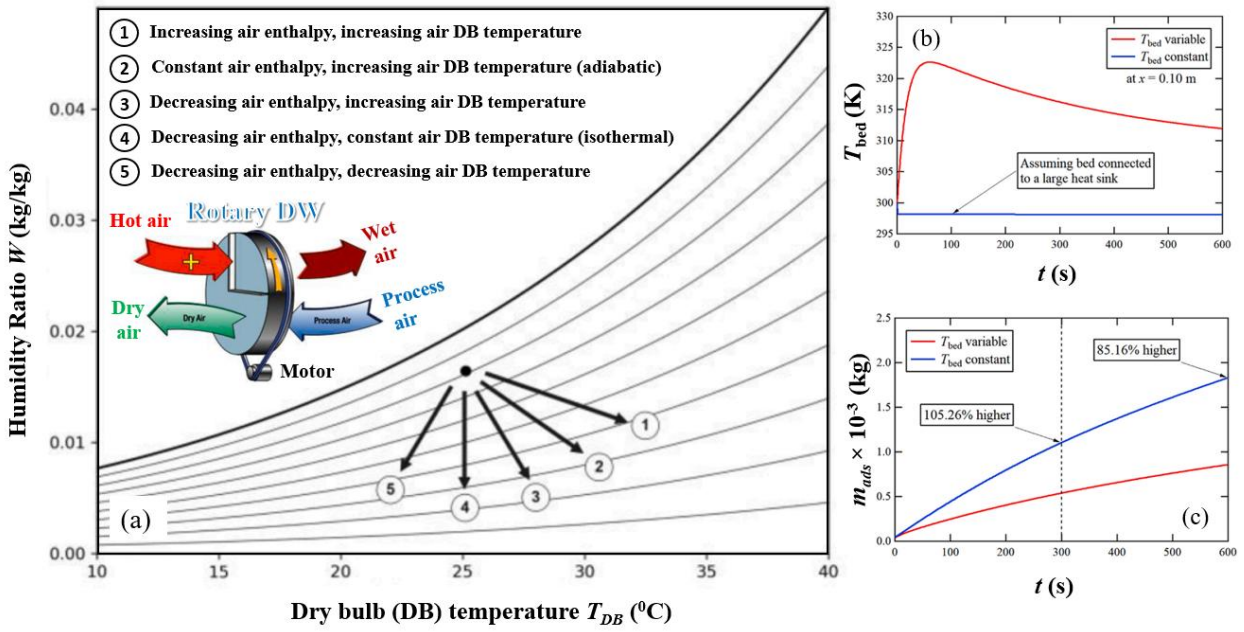

Figure 6. Influence of internal cooling on the dehumidification performance. (a) Psychometric representation of different dehumidification scenarios in a DW [23], (b) Illustration of desiccant bed temperature in an MFBDD device for non-isothermal and isothermal cases [4], and (c) Mass of water adsorbed in an MFBDD device when bed temperature is constant (isothermal) and variable (non-isothermal) [4]. DB represents dry-bulb temperature in Figure 6a.

To achieve isothermal dehumidification in DWs, internal cooling using additional flow channels, through which a cold working fluid is supplied to remove the enthalpy of adsorption, is used. Numerical studies have demonstrated the improved performance of systems that are internally cooled [47-49]. However, internal cooling methods are easier to use with desiccant-coated heat exchangers because of their stationary configuration and reduced leakage risks [50-

53]. **Table 1** summarizes the studies evaluating the dehumidification performance of DWs with single-stage internal cooling. However, a major drawback of using internal cooling in DWs is that it lowers the moisture transfer area and reduces dehumidification capacity. Hence, additional flow channels should be added, but they would make the system more complex and enhance the chance of leakage. Another concern associated with internal cooling is the additional pumping power required for circulating water, as well as energy input for the cold working fluid.

Table 1. Studies evaluating the dehumidification performance of DWs with single-stage internal cooling.

Ref.	Configuration and research highlights
[49]	• Alternative rectangular channels carried regeneration heat from the desiccants **(Figure 7a)** • Dehumidification capacity improved by 45%–53% • Crossflow arrangement was less effective than counterflow arrangement
[54]	• The DW used counterflow cooling water channels **(Figure 7b)** and was made of nylon and polymer materials • Compared with conventional wheels, the DW demonstrated a ~11% increase in enthalpy effectiveness
[48]	• A stationary central shaft connected the wheel to circulating cooling water, which flowed into the tubes and was collected in the liquid shell **(Figure 7c and 7d)** • Process and regeneration airstreams flow through the upper and lower halves, respectively • The wheel was made from PVC, and silica gel was the desiccant used • Compared with a conventional wheel, the proposed configuration showed a 40% improvement

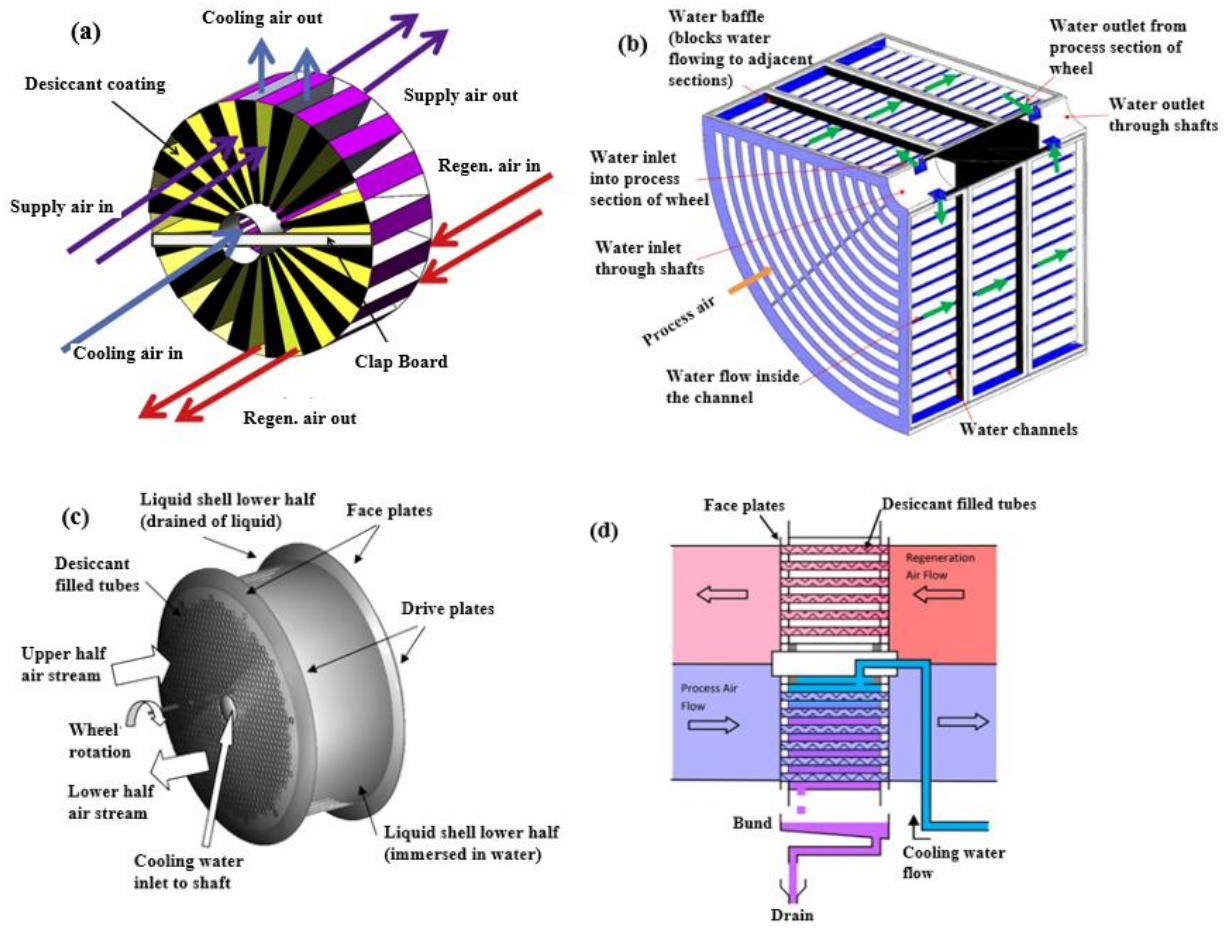

Figure 7. Internal cooling arrangements of DW proposed by different researchers. Internally cooled DW configurations proposed by (a) Narayan et al. [49], (b) Zhou and Reece [54], (c) Goldsworthy and White (3D view) [48], and (d) Goldsworthy and White (cross-section view) [48].

ii) Multistage with interstage cooling

Multi-stage DWs use two or more wheels to dehumidify air in series with interstage cooling or heat sources placed between the wheels. The interstage cooling reduces the temperature increase in the process air stream, which enables maintaining a high difference in vapor pressure between the airstream and desiccants. Multi-stage DW systems has the potential to improve the dehumidification efficiency, reduce the regeneration temperature, and make the system feasible for low -grade waste heat or renewable heat integration. Infinite multi-stage cooling is similar to internal cooling technology, aiming to bring the air dehumidification process closer to the isothermal line. Shahvari et al. [55] compared four DW configurations with silica gel and MOFs as shown in **Figures 8a through 8d**. The authors proposed using different MOFs in the four-stage

configuration to cover different RH ranges. Their results showed that MOF-based multi-stage DW achieved 20%–40% higher dehumidification efficiency compared with the single-stage system. However, the when the system expanded beyond four stages, the benefits of the multi-stage system diminished.

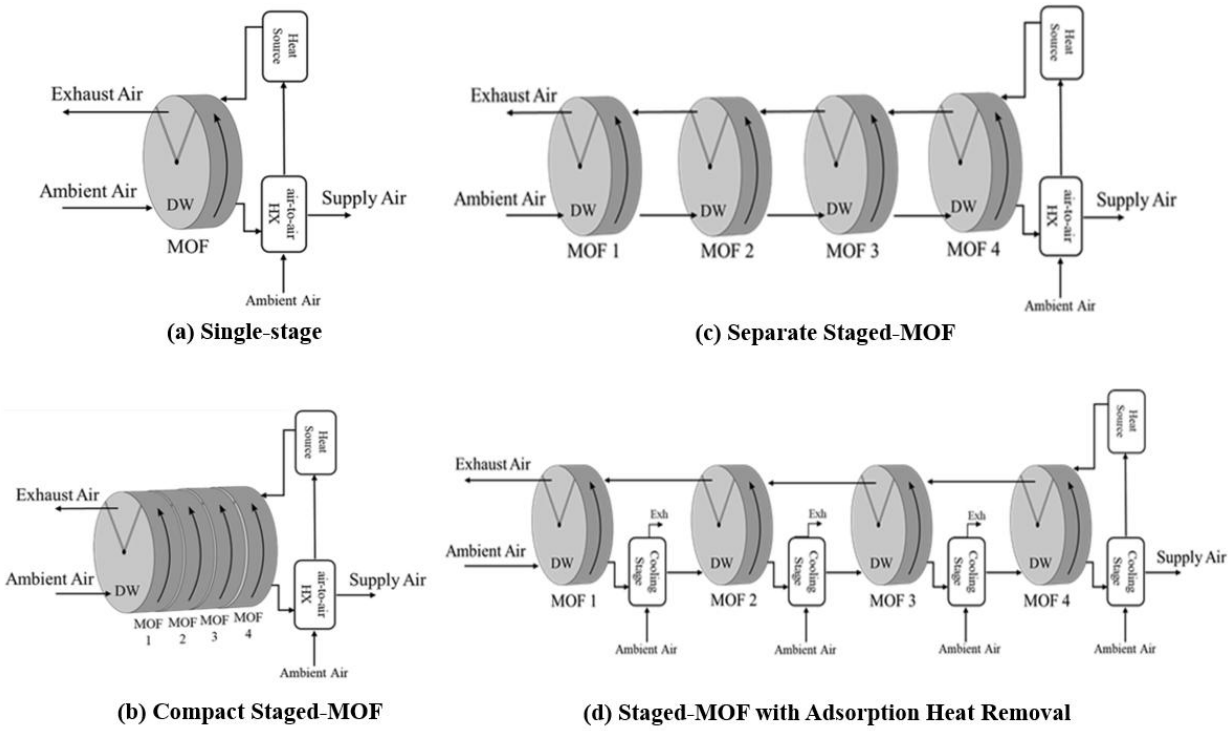

Figure 8. DWs with different interstage cooling arrangements. (a) Single-stage cooling, (b) Compact multi-stage cooling, (c) Separate multi-stage cooling, and (d) Separate multi-stage cooling with enthalpy of adsorption removal [55].

3.2 Performance Metrics for DWs

Comparisons of the performance of air dehumidifiers are challenging since existing publications do not use the same testing conditions and performance parameters. **Table 2** summarizes the commonly used performance metrics to evaluate a rotary adsorption device for gas removal [ref]. In the later part of this review article, the performances mentioned are refer to the equations provided in this section for better consistency and comparison.

Table 2. Summary of performance metrics for air dehumidifiers

Performance metric	Equation	Unit	Description
Dehumidification capacity (*DC*)	$\Delta\omega = \omega_{pa,in} - \omega_{pa,out}$ (Eq. 1)	g/kg$_{DA}$	Reduction of specific humidity between process air (*pa*) in and out
Dehumidification effectiveness (ε)	$\varepsilon = \frac{\omega_{pa,in} - \omega_{pa,out}}{\omega_{pa,in}}$ (Eq. 2)	—	Ratio of reduction of specific humidity to air specific humidity
Moisture removal capacity (*MRC*)	$MRC = \dot{m}_{pa}\left(\omega_{pa,in} - \omega_{pa,out}\right)$ (Eq. 3)	g/s	Amount of moisture removed per unit of time
Moisture removal efficiency (*MRE*)	$MRE = \frac{MRC}{\dot{Q}_{reg}}$ (Eq. 4)	g/s/KW	Ratio of the moisture removal capacity (g/s) to the power input for regeneration (KW)
Cooling COP (COP_C)	$COP_C = \frac{\dot{Q}_c}{\dot{Q}_{reg}}$ (Eq. 5)	—	Ratio of cooling capacity of the cooling system to the regeneration heat input
Dehumidification COP (*DCOP*)	$COP_{lat} = \frac{\dot{m}_{pa}(\omega_{pa,in} - \omega_{pa,out})h_{lat}}{\dot{Q}_{reg}}$ (Eq. 6)	—	Ratio of latent heat in adsorbed moisture to thermal energy delivered to regeneration air
Regeneration efficiency (η_{reg})	$\eta_{reg} = \frac{\dot{m}_{pa}(\omega_{pa,in} - \omega_{pa,out})h_{lat}}{W_{reg}}$ (Eq. 7)	—	Ratio of moisture removal rate multiplied by heat of evaporation divided by the regeneration power
Regeneration specific heat input (*RSHI*)	$RSHI = \frac{\dot{Q}_{reg}}{\dot{m}_{PA}(\omega_{pa,in} - \omega_{pa,out})}$ (Eq. 8)	kJ/kg	Ratio of regeneration power to moisture removal capacity

3.3 Advances in Desiccant Materials for DW

Developing new desiccant materials that possess the desired characteristics, is pivotal to enhancing the dehumidification performance of DWs. The ideal adsorbents for dehumidification application should have the following characteristics:

- Steep or stepped isotherm (Type IV or V) with uptake steps occurring near and below the recommended indoor range (e.g., 40%–60% RH)
- Large capacity for uptake of gases (e.g., water vapor)
- Stability under the long-term adsorption and desorption cyclic operations
- No or small hysteresis between the adsorption and desorption isotherms
- Good kinetics for fast adsorption and desorption
- Good sorbent scalability
- High selectivity for water vapor
- Low pressure drops and high surface area contactor
- Low-cost energy sources for adsorbent regeneration
- Acceptable capital cost and long-term performance of desiccants

Although a wide range of solid desiccants are investigated in the literature, the three recent generations of porous materials include metal-organic frameworks (MOFs), superabsorbent polymers (SAPs), and thermo-responsive hydrogels. Since previous reviews [28, 56, 57] have extensively discussed the commonly used conventional solid desiccants (e.g., silica-gel, carbon, and zeolite-based), this article focuses on the new generation desiccants only.

i) MOFs

MOFs are the most promising porous materials for various heat and moisture transfer applications, including dehumidification [58], adsorption heat pumping [59], and water harvesting [60]. Typically, MOFs comprise metal centers and organic linkers. Their structures can be controlled by selecting appropriate organic ligands and metal ions, which gives flexibility to tailor their key thermophysical properties (e.g., porosity, pore size distribution, and thermal conductivity) for specific applications. The superiority of MOFs comes from their high surface area (~ 3,000 m^2/g), stability at high temperature (>400°C), and flexibility of functionalization [61-63], which makes them excellent candidates for dehumidification applications. Karmkar et al. [58] reviewed an extensive catalog of MOFs as energy-efficient desiccants in various applications. This section reviews the recent progress on the application of MOFs with DWs for dehumidification application.

Figure 9a and 9b compare the water uptake capacity of the MIL series of MOFs with that of traditional adsorbents (silica gel–based and zeolite-based). Some MOFs exhibit high water adsorption capacity, such as MIL-101(Cr)@GO, which has a capacity up to 1.6 kg/kg (**Figure 9a**). In contrast, the maximum water uptake capacity of traditional adsorbents is limited to 0.35 kg/kg, which is almost 4.6 times lower **(Figure 9b**). A more rigorous database for the moisture adsorption capacity of various MOFs suitable for air-conditioning application is available in the review of Liu et al. [64]. Another advantage of using MOFs is that they show a step-like isotherm, unlike traditional adsorbents, which can significantly enhance the dehumidification ability of the DW if the outdoor air RH lies within the same range as the step location of the isotherm. Bezrukov et al. [36] assessed the potential of seven MOFs for ambient water harvesting applications as shown in **Figure 9c.** Among the investigated MOFs, two were termed as regeneration-optimized sorbent (ROS) (ROS-037 and ROS-039), as these MOFs exhibited high uptake, fast desorption and low heat input for regeneration.

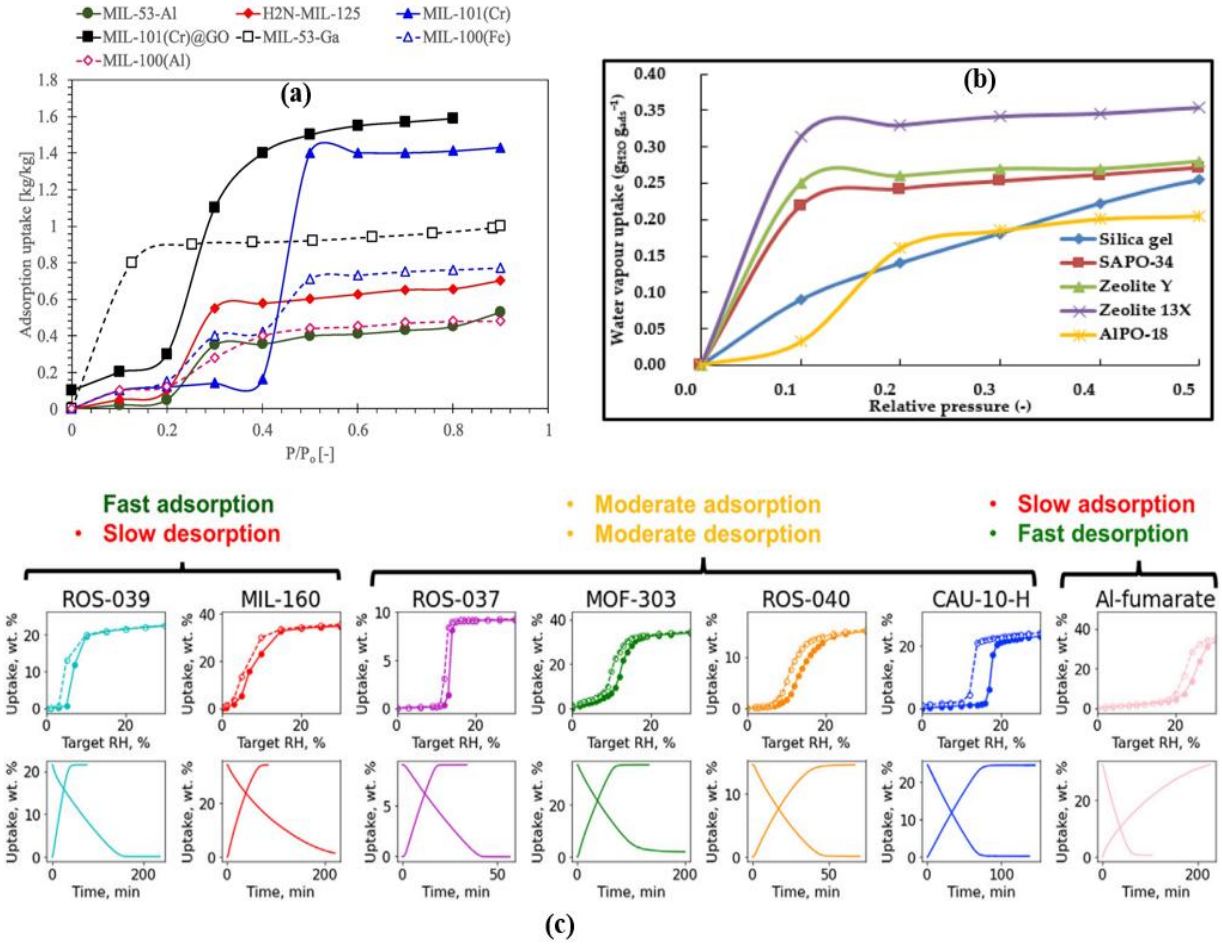

Figure 9. Water vapor adsorption isotherms, uptake and release capacities different MOFs and conventional adsorbents. Water vapor uptake capacity of (a) MIL series MOFs [65], (b) Traditional adsorbents [66], and (c) Adsorption isotherms and water vapor uptake and release capacities of seven different MOFs studied by Bezrukov et al. for water harvesting application [36]. ROS represents regeneration optimized sorbent.

Several other recent studies in the literature have also investigated the dehumidification performance various MOFs in DW. A summary of these studies is given below in **Table 3.**

Table 3. Studies investigated MOFs as a desiccant for air dehumidification in DWs.

Ref.	MOFs investigated	Research highlights
Azizv et al. (2022) [67]	CPO27(NI), MIL100(Fe), MIL-101(Cr), Aluminium Fumarate, Base case desiccant: Silica gel	• A stationary DW was numerically modeled in 1D and validated. • Numerically obtained COP and moisture removal capacity (MRC) (g/kg) were in the order of Aluminum fumarate> MIL-101(Cr)> MIL100(Fe)> CPO27(NI)> Silica gel. • Velocity of incoming air significantly affected the MRC, and the MRC reached the peak value within the first two minutes of adsorption process.
Liu et al (2022) [68]	Aluminum Fumarate Base case desiccant: Silica gel	• The dehumidification capacity (DC) and COP of MOF-based DW were significantly higher (DC 40-48% and COP 13-19%), than that of the DW impregnated with silica-gel. • Compared to silica gel based DW, the MOF-based DW exhibited low temperature rise when ambient humidity ratio was low, and low temperature rise when ambient humidity ratio was high, at 50 ^{o}C regeneration temperature.

Park et al. (2023) [69]	MIL-100(Fe) Base case desiccant: Silica composite	• The MOF-based DW exhibited sensible energy ratio as low as 53% and specific moisture removal capacity as high as 139% than that of silica composite DW. • The influence of altering various operating parameters (e.g., temperature, relative humidity, process air flow velocity, and heat input for regeneration) were investigated. • The optimum rotational speed for MOF-based DW was 40 rev h^{-1}, resulted in moisture removal rate of 1.97 kg h^{-1}.
Shahvari et al. (2022) [70]	10 different MOFs having steep isotherm Base case desiccant: Silica gel	• A first-principles-based numerical model for a DW was developed and validated with experiment. • The best performing MOFs were Co_2Cl_2(BTDD), Al-fumarate and CAU-23, as their regeneration temperatures were as low as 40-60 ^oC, whereas for silica gel it was 80-140 ^oC. • Because of the steep water uptake isotherm, MOF DWs could remove more moisture than silica gel DW and resulted in greater regeneration efficiency.
Shahvari and Clark (2023) [55]	CAU-10(Al), CAU-23(Al), MIL-125-NH2(Ti), MIL-125	• A multistage MOF DW system was proposed based on the idea that there exists an optimal MOF for each stage as a function of inlet air properties. • Multistage system exhibited 5-20% higher regeneration efficiency and 20-40% higher dehumidification effectiveness than that of single stage system. • Multistage system has the ability to reach the theoretical limit for dehumidification, corroborating

		the high energy-saving potential of the multistage system.
Shahvari et al. (2022) [71]	Co_2Cl_2(BTDD)(Co), Al-fumarate(Al), or CAU-23(Al) Base case desiccant: Silica gel	• Performance of a MOF-based DW combined with indirect evaporative cooler was numerically investigated using a first principles based model and mimicking variety of outdoor conditions. • The results showed that MOF-based DWs could obtain 2.7 ~ 6 times higher COP compared to silica gel DW. • The optimal regeneration temperature for MOF DWs lied in the range 40 to 75 °C, demonstrating the potential of integrating low-temperature heat sources for regeneration.

ii) SAPs

SAPs are cross-lined polymer networks made from water soluble monomers. These polymers, mostly comprising ionic monomers with relatively low crosslinking density, can absorb water up to 1,000 times their own weight [72]. An illustration of different subdivisions of SAPs is shown in **Figure 10.**

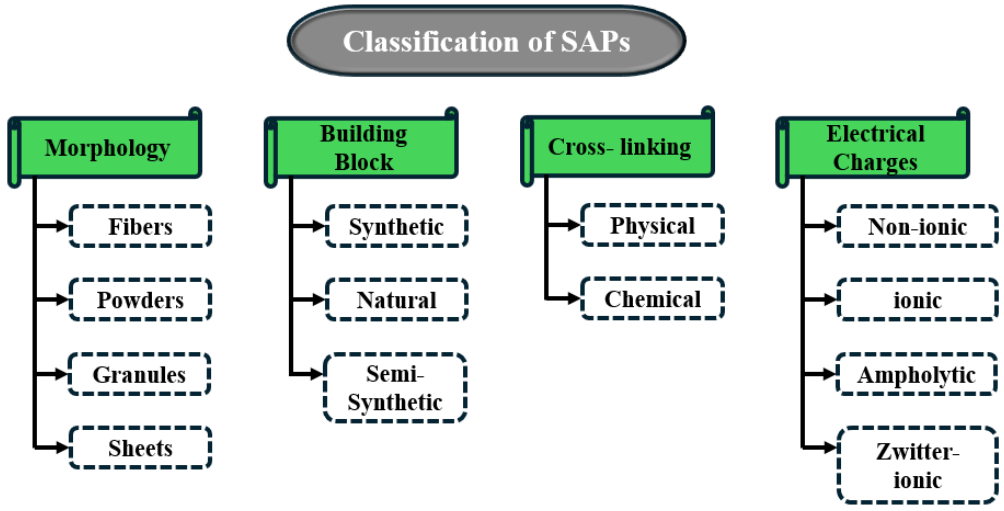

Figure 10. Subdivisions of SAP classifications [72].

Lee and Lee [73] studied the water vapor adsorption isotherm and diffusivity in super desiccant polymer (SDP). Their results revealed that 67% relative humidity the water uptake of SDP was 128%., and the diffusivity spanned between 6.4×10^{-13} to 5.9×10^{-11} m^2/s. The SDP coated wheel also exhibited excellent hydro-thermal stability during 40000 cycles adsorption-desorption operation. Higashi et al. [74] reported that the mass diffusion coefficient of SAPs is 1–2 orders of magnitude greater than that of silica gel. Although SAPs have shown promise as desiccant materials and have been experimentally evaluated in desiccant-coated heat exchangers [20], their use in DWs remains limited. **Table 4** summarizes the studies evaluating the dehumidification performance of SAPs with DWs and packed bed dehumidifier.

Table 4. Studies evaluating the dehumidification performance of various SAPs in DWs and packed bed.

Ref.	Types of SAPs	Device Type	Research highlights
White et al. (2011) [75]	Polyacrylic acid salt	DW	• At a low regeneration temperature (50°C) and high relative humidity (>60%), DWs with SAPs demonstrated a 10%–15% higher dehumidification capacity than silica gel • The SAP DW did not significantly benefit from increasing the regeneration temperature (80°C) • Despite the SAP's equilibrium, moisture absorption capacity was 4–5 times that of silica gel; the differences in dehumidification performance between them were surprisingly minor • Higher uptake alone cannot ensure high system performance; isotherm shape and point of inflection are also crucial parameters to enhance the overall system performance

Kang and Lee (2017) [76]	Super desiccant polymer	DW	• Three DWs were tested with varying wheel thicknesses and desiccant contents under different air velocities and rotation speeds • The super desiccant polymer wheel exhibited better dehumidification with a small sensible temperature rise compared with conventional desiccants
Chen et al. (2015) [77]	Polyacrylic acid and sodium polyacrylate combined with varying ratios of silica gel	Packed Bed	• Adsorption capacity of the composite desiccant increased with a higher proportion of sodium polyacrylate, and for the ratio 10:5, uptake capacity was 17% higher than that of silica gel • Higher sodium polyacrylate ratios made the composite softer to utilize after absorbing water • Introducing a small proportion of polyacrylic acid to the composite resulted in remarkably high adsorption capacity • Excessive swelling of SAP desiccants can contract air passages, leading to high pressure drop, and can make the desiccant prone to breaking

iii) Thermo-responsive hydrogels

Thermo-responsive hydrogels displays a switchable transition between hydrophilic behavior when exposed to humid air, and hydrophobic behavior when exposed to heat. This conversion is accomplished through temperature-responsive (TR) polymers with a low critical solution temperature (LCST). Below the LCST, the polymers are relatively hydrophilic, whereas above it, they become hydrophobic [41]. This property enables the formation of a temperature-dependent adsorption isotherm. Consequently, the material can absorb water vapor from process airstream and release it more efficiently when heated by regenerated airstream above the LCST. The thermo-responsive hydrogel is an interpenetrating polymer network gel comprising a TR polymer and

hydrophilic sodium alginate networks. **Figure 11a** shows the water vapor uptake and release mechanism in a thermos-responsive polymer, and **Figure 11b** shows the amount of water collected in 24 hours by super moisture-adsorbent gel developed by Zhao et al. [78].

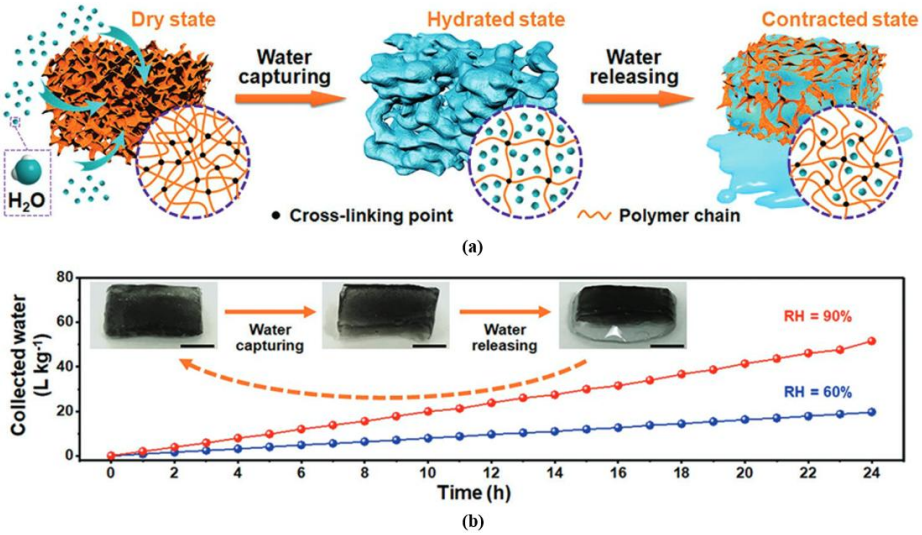

Figure 11. Water vapor uptake and release mechanism in thermos responsive polymers. (a) Illustration of atmospheric water vapor adsorption and desorption in a super moisture-adsorbent gel when exposed to humid air and heat, and (b) Atmospheric water collection at different humidity levels in 24 h using a super moisture-adsorbent gel developed by Zhao et al. [78].

Albeit thermos-responsive hydrogels have great potential for dehumidification applications, at present their applications are mainly limited to atmospheric water harvesting [78, 79]. Charles [80] developed a hygroscopic salt–impregnated, N-isopropylacrylamide (NIPAM) hydrogel–based thermo-responsive desiccant material and studied the suitability of this material for dehumidification application. The proposed material achieved swelling ratio >2, and it could be regenerated with low heat input as compared to conventional desiccants. Zeng et al. [81] computationally demonstrated that TR polymers can reduce the energy cost of dehumidification systems that employ DWs by 17%–30%. Dehumidification efficiency can be further enhanced by modifying the isotherm and LCST of TR polymers for different applications. For instance, lower LCST is beneficial to HVAC supply air streams, and higher LCST is advantageous for ventilation air. Meyer et al. [41] noted that the main challenge in developing effective TR polymer desiccants lies in concurrently meeting the following conditions: maintaining the TR attributes of the polymer, integrating hydrophilic elements for controlling a medium thermo-responsiveness, and achieving

consistent cycling performance. Although the polymer structure improves the desirable properties of TR polymer desiccants, substantial work is required to address issues such as salt leaching and realizing liquid water release.

iv) Dehumidification and regeneration performance analysis of MOFs and SAPs based DWs

This section provides a summary of the dehumidification and regeneration performance of MOFs and SAPs based DWs. The regeneration efficiency and regeneration temperature of ten different MOFs was compared by Shahvari et al. [70] as shown in **Figure 12.** The four best MOFs exhibited highest efficiency and lowest regeneration temperature are: MOF-841, Aluminum-Fumarate, Co2Cl2(BTDD) and CAU-23. **Table 5** summarizes the operating conditions and dehumidification performance of MOFs and SAPs with DWs as reported in the studies listed in **Table 3** and **Table 4,** respectively. To be noted that different studies have reported dehumidification performance using different performance indicators. The operating conditions and physical dimensions of the DWs of these studies also vary significantly from one to another. Therefore, it is difficult to directly compare the outcomes of these studies. However, in general from **Table 5** we can see that MOF-based DWs exhibited higher dehumidification performance and lower regeneration temperature as compared to silica gel-based DWs.

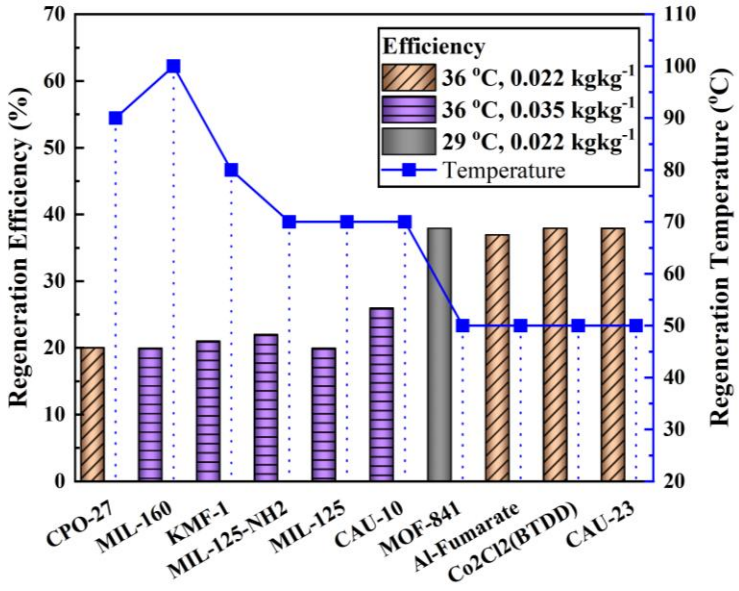

Figure 12. Regeneration efficiency and regeneration temperature of ten different MOFs in a DW as compared by Shahvari et al. [70].

Table 5. Summary of operating conditions and dehumidification performance of MOFs and SAPs when employed in DW.

Source	Method	Device Type and Size (cm)	Adsorbent Type	Supply Air Properties			Regen. Air Temp. (℃)	Rotation Speed (rev/hr)	Dehumidification Performance			
				Sp. Humidity (g/kg)/ Rel. Humidity (%)	Temp. (℃)	Face Vel. (m/s)			DCOP	DC (g/kg)	Effect. ε	MRC (kg/hr)
Shahvari and Clark (2023) [55]	Modeling	DW (dia.: 50)	Type V Isotherm	10-30	27-33	2.8	80-95	NA	NA	NA	0.71 (Confg. 1), 0.26-0.53 (Confg. 2), 0.26-0.50 (Confg. 3) **(Note 6)**	NA
Azizv et al. (2022) [67]	Modeling and Experiment	Stationary Wheel (dia.: NA)	Silica Gel, Al-Fumarate, MIL00(Fe), MIL-101(Cr), CPO27(NI)	17	30	1.5-3.1	70	Stationary	0.36 (SG), 0.39-0.65 (MOF)	5.26 (SG), 6.55-15.98 (MOF)	NA	NA
Liu et al (2022) [68]	Experiment	DW (dia.: NA)	Silica Gel, Al- Fumarate	7.06-21.57	22-30	2.3-3.2	50-90	7.73-14.35	0.24-0.53 (SG), 0.31-0.72 (MOF)	2.07-2.69 (SG), 2.51-3.38 (MOF)	NA	NA
Park et al. (2023) [69]	Experiment	DW (dia.:48.2)	MIL-101(Fe)	8-12	15-25	NA	55-65	10-60	0.11-0.32 **(Note2)**	NA	NA	0.99-2.08

Shahvari et al. (2022) [70]	Modeling	DW (dia.: 32)	Silica gel, MIL-125-NH2(Ti), MIL-125(Ti), MOF-841 (Zr), CPO-27(Ni), Co2Cl2(BTDD) (Co)	15-35	29-36	NA	40-60 (MOF), 80-140 (SG)	NA	NA	NA	NA	NA
Shahvari et al. (2022) [71]	Modeling	DW (dia.: 50)	Silica gel, CAU-10(Al), CAU-23(Al), Co2Cl2(BTDD)	15-35	25-40	2.8	40-75 (MOF), 55-150 (SG)	NA	0.32-1.49 (CAU-23), 0.25-1.43 (Co2Cl2(BTDD)), 0.23-0.85 (CAU-10), 0.19-0.64 (SG) **(Note3)**	NA	NA	NA
White et al. (2011) [75]	Experiment	DW (dia.: 36 & 30)	Silica gel, Zeolite (FAM-Z01), SAP	20-90%	20, 30	1.7, 2.5	50, 80	20 (Optimum)	NA	2.54-5.29 (SG), 2.24-6.05 (Zeolite), 1.05-5.58 (SAP) **(Note 4)**	NA	NA

Kang and Lee (2017) [76]	Experiment	DW (dia.: 58)	SAP	13.2	32	1.0-2.4	60	NA	NA	3.72 **(Note 5)**	0.432 **(Note 5)**	NA
Chen et al. (2015) [77]	Experiment	Packed Bed	Comp. Desiccant **(Note1)**	60-80%	20, 30	2.0-3.0	50, 60	NA	NA	NA	NA	0.17 **(Note 7)**

NA: Not Available; **SG:** Silica gel;

Note 1: Silica gel, polyacrylic acid and sodium polyacrylate, with optimized mass ratios 10:1:1);

Note2: at regeneration temperature 50 ℃, 40 rev./hr, supply air sp. humidity 10 g/kg, and supply air temp. 15-25 ℃.

Note3: at supply air sp. humidity 15 g/kg, and supply air temp. 29 ℃.

Note 4: at regeneration temperature 80 ℃, supply air face vel. 2.5 m/s, and supply air temp. 20 ℃.

Note 5: for wheel #1, 200 sec cycle time and 2.4 m/s face velocity.

Note 6: supply air sp. humidity 30 g/kg

Note 7: 10 min average, at regeneration temperature 40 ℃, supply air RH 70%, supply air temp. 30 ℃., supply air face velocity 2 m/s.

v) Influence of operating conditions on dehumidification with DW

The typical operating parameters considered in the dehumidification process include the inlet air temperature, humidity, wheel rotational speed, the desiccant material used, wheel flow channel geometry, regeneration temperatures, and airflow rates [82-88]. Nia et al. [43] investigated the influence of various operating conditions on dehumidification effectiveness and process outlet air temperatures. Through numerical modeling, they determined that there is an optimal rotational speed, air channel height, and desiccant-coated substrate thickness at which effectiveness is maximized. Additionally, they reported that as the inlet humidity ratio, temperature, and air flow rate or velocity increase, effectiveness also increases. These findings also align with other numerical studies that evaluate the effects of operating conditions on wheel performance [84, 88].

DCOP, MRC, and pressure drop are other key performance indicators for DWs. A recent study by Park et al. [89] on MOF-based DWs examined the effects of rotational speed, inlet humidity ratio, and regeneration temperature on MRC and DCOP. Key findings from this study include the identification of a limiting rotational speed at which MRC and DCOP are maximized as shown in **Figure 13a.** This limitation may be due to incomplete regeneration, as higher rotational speeds can reduce dehumidification performance. The parametric study also reported that the DCOP increases with increase in inlet humidity, possibly due to the fact that amount of processed water vapor during dehumidification get increased at same regeneration heat. **Figure 13b** shows the variation in DCOP as a function of absolute humidity at two different process air inlet temperatures. In addition to the performance parameters discussed above, the effect of regeneration angle was reported by Muthu et al [86]. For a given set of input conditions, there exists an optimal combination of regeneration angle and regeneration air inlet temperature, at which the moisture carrying capacity reaches its maximum. Beyond this optimal regeneration angle, increasing the angle further does not lead to any additional increase in the moisture removal capacity of the process air.

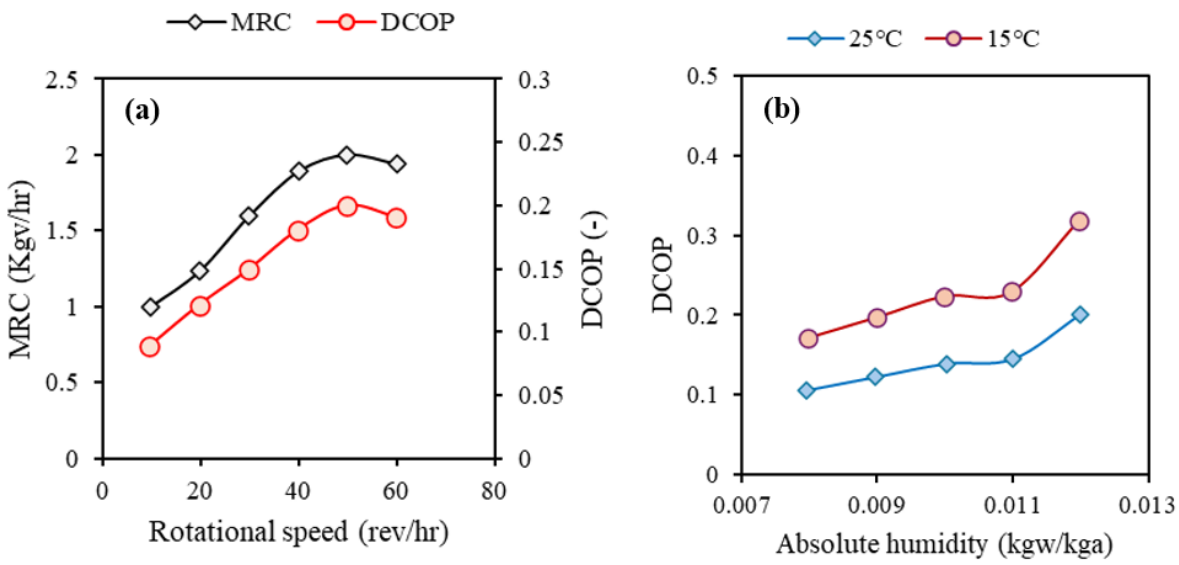

Figure 13. Influence of operating conditions on the performance of DW. (a) MRC and DCOP as a function of rotational speed. Flow rate and temperature (process/regeneration side): 600 m3/hr /600 m^3/hr and 20°C/55°C, and (b) DCOP as a function of absolute humidity at 15°C and 25°C process air inlet temperature. Process/regeneration side flow rate: 600 m3/hr and rotational speed: 40 rev/hr and regeneration temperature: 55°C.

3.4 Advances in System-level Performance Evaluation with DWs

i) DWs coupled with electrically driven heat pumps

The International Energy Agency has identified electrifying heat in the built environment using heat pumps and phasing out combustion-based heating appliances as top priorities [90]. These goals led to the installation of 177 million heat pumps in 2020 [91]. To achieve the International Energy Agency's clean energy goals for the built environment, 600 million heat pump units will be required by 2030 globally. This effort highlights the opportunity to combine DWs with heat pumps for simultaneous dehumidification and cooling in summer operations with enhanced energy efficiency.

The basic configuration of a typical vapor compression heat pump is illustrated in **Figure 14a;** it comprises a compressor, a heat sink for the refrigerant (condenser), an expansion valve, and a heat source for the refrigerant (evaporator) [23]. In a coupled heat pump DW (HPDW) system, the refrigerant's phase change heat available at the condenser can be used during the summer for regeneration purposes, and the cooling effect available at the evaporator can be used

for cooling of the process air. Coupling a DW with a vapor compression heat pump can be done in two ways [27]: (1) when the evaporator provides pre-cooling of the process air prior to entering into the DW **(Figure 14b),** and (2) when the evaporator provides post-cooling of the dehumidified process air leaving the DW and entering the conditioned space **(Figure 14c). Figure 14d** illustrates the psychrometric representation of these two configurations. The cooling desiccant configuration can achieve a higher dehumidification capacity, but the outlet air temperature remains high and cannot meet the indoor temperature requirement [27]. **Table 6** summarizes the studies evaluating the performance of DWs coupled with electrically driven heat pumps.

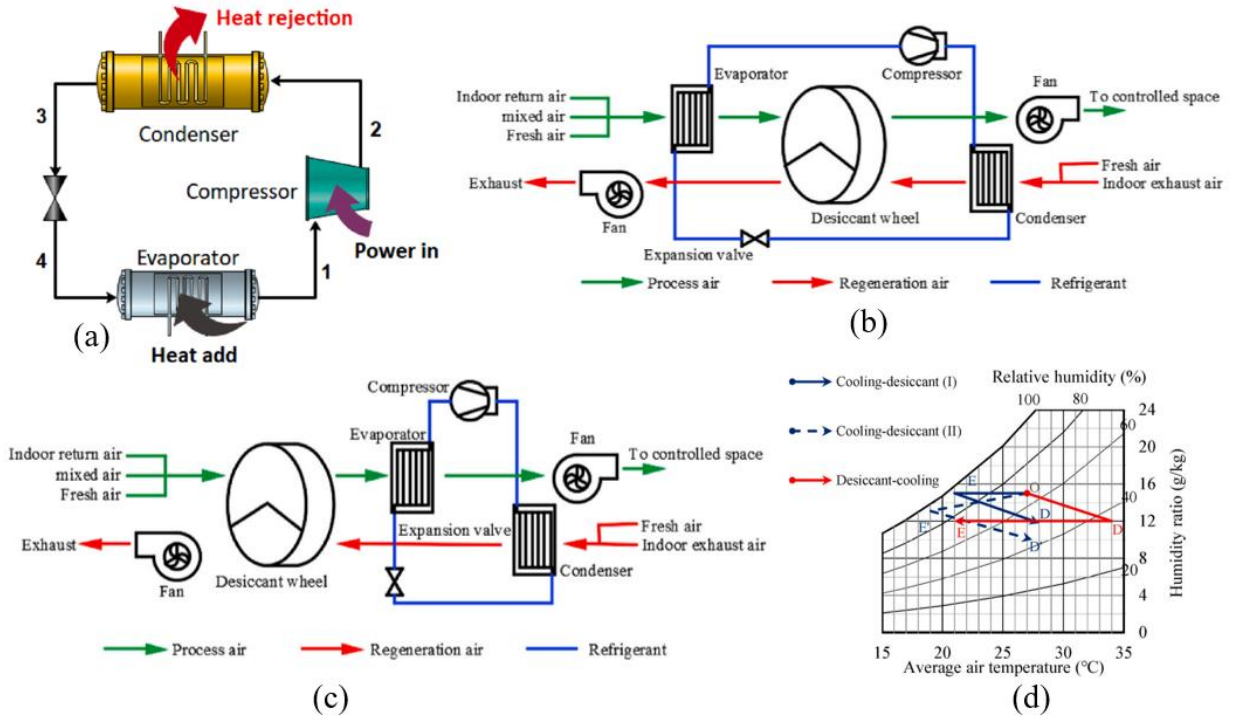

Figure 14. Schematic of HPDW combined with vapor compression heat pump system. (a) Typical vapor compression system [23], (b) HPDW with the evaporator for pre-cooling [27], (c) HPDW with the evaporator for post-cooling [27], and (d) Psychrometric representation of the cycles illustrated in (b) and (c) [27].

Table 6. Studies evaluating the performance of DWs coupled with electrically driven heat pumps.

Ref.	Type of study	Research highlights
[92]	Modeling	• An HPDW system was analyzed for an office building in Istanbul during working hours using R32, R1234yf, R290, R134a, R600a, R245fa, and R717 for the vapor compression system • The effect of the different refrigerants on energy and exergy performance was evaluated • Without a DW, R1234yf consumed the highest power and R717 consumed the lowest. With the effectiveness of a DW, energy consumption with R1234yf was reduced. Considering total electricity consumption, R717 showed the best energetic and exergetic performance
[93]	Modeling	• A HPDW system consisted of two heat pump systems, a high-temperature heat pump system for regeneration ($HTHP_{reg}$) and an auxiliary heat pump system for process air (HP_{prcs}) • By combining two sub-systems ($HTHP_{reg}$ and HP_{prcs}) deep dehumidification could be achieved, with dehumidification efficiency between 2.05 to 2.67 kg/kWh • HP_{prcs} reduces the regeneration heat load of a DW by 20% and enhances seasonal moisture removal efficiency by 13% to 17%. However, equipment cost is 68% higher for this system, while the cost of primary energy is reduced by 42% than that of a DW without HP_{prcs} due to enhanced performance, resulting in a 27% lower levelized cost with a payback period of 2.81 years
[94]	Modeling	• Performance a solar desiccant cooling system (a.k.a. HP-PSDC) was evaluated for the cases when it was operated with a heat pump and

		when without a heat pump. The HP-PSDC system utilized phase change material to enhance the efficiency. • The performance evaluation of the HP-PSDC system was carried out under typical weather conditions in the following four cities: Doha, Vancouver, Toronto, and Bangkok • The HP-PSDC system exhibited high COP in all four weather conditions. However, the operation with heat pump was found to be more efficient as the wet-bulb temperatures exceeded 21.5°C. For the wet-bulb temperatures below 18.5°C, operation without utilizing heat pump was found to be more favorable.
[95]	Experiment	• HPDWs with two-stage evaporation (pre-cooling and indoor evaporator), two-stage condensation, and two-stage dehumidification were evaluated, and benchmarked with that of a single-stage DW. • The two-stage dehumidification system exhibited higher efficiency in terms of energy savings for the following cases: RH below 49% at high temperature mode, RH below 55% under the typical summer conditions, and RH below 40% for the dehumidification mode.
[96]	Experiment and modeling	• An HPDW with two-stage evaporation (pre-cooling and indoor evaporator) and two-stage condensation for nZEB was evaluated • Optimized the pre-cooled process air temperature at the outlet of the evaporator, and the performance of the HPDW system was compared with a typical air-conditioning unit • The pre-cooling of process air at optimal temperature ensured that the indoor RH maintained lower than 70% for more than 96% of the time.

		• The energy benefits (savings) achieved by the HPDW system was 9.4% higher during the summer operation, and 14.9% higher for dehumidification compared to the typical air-conditioners.
[97]	Experiment and modeling	• An internal heat exchanger provided pre-cooling for process air (after dehumidification and before passing over the evaporator) and pre-heating for regeneration air (prior to passing over the condenser) • The performance of a heat pump condensing dehumidifier (air dehumidified below the dew point) and an HPDW was compared. • The condensing dehumidifier exhibited 3–4 times higher exergy efficiency than HPDW.

ii) DWs coupled with ground-source heat pumps

Ground-source heat pumps (GSHPs) can be alternatives to air-source heat pumps when combined with DWs. In a GSHP, the evaporator is usually connected to the ground, which acts as the heat source or sink. GSHPs are advantageous over air-source heat pumps because of their greater underground thermal stability compared with seasonal and daily air temperature variations, and their lack of need for defrosting in winter [98]. However, GSHP requires higher installation costs and a longer payback period than air-source heat pumps. **Figure. 15** illustrates the schematic of a DW coupled with a GSHP and solar collector, where the GSHP can be utilized to precool the process air before it passes through the DW and post-cool the dehumidified air in order to maintain adequate thermal comfort. **Table 7** summarizes the studies evaluating the performance of DWs coupled with GSHPs.

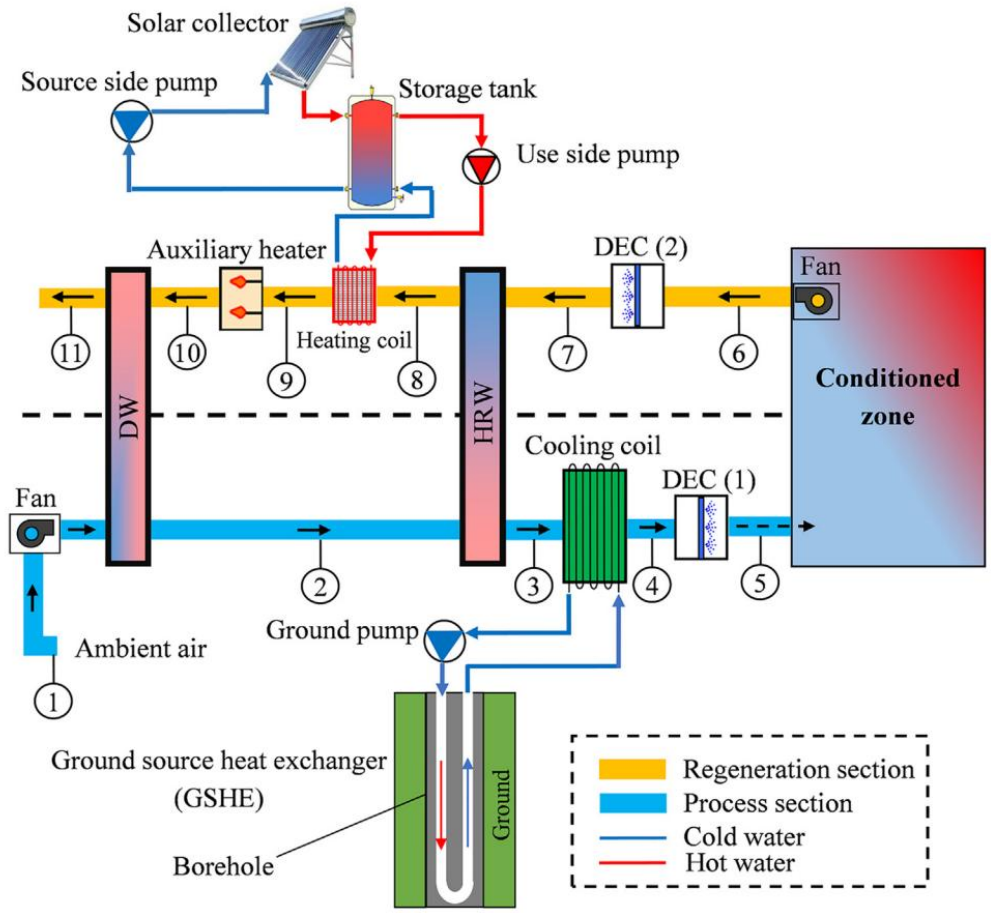

Figure 15. Schematic of a DW coupled with a GSHP and a solar collector [99].

Table 7. Studies evaluating the performance of DWs coupled with GSHPs.

Ref.	Research highlights
[100]	• A hybrid ground-assisted desiccant cooling system (HGDC) was examined • The HGDC had a 7.7%–31.75% lower power consumption compared with a conventional vapor compression system during the summer • Pre-cooling of process air by the GSHP accounted for nearly 33%–73% of the total cooling load • A COP of 4.10 was achieved under the specified outdoor conditions (air temperature of 33.3°C and humidity of 24.9 g/kg)

[101]	• The performance of a desiccant cooling system combined with solar and ground-source free cooling was examined • The proposed system ensured thermal comfort during 95% of its operating hours and achieved a COP of 0.43. In the best case scenario, the payback period for the proposed system was estimated as 6.8 years
[99]	• Multi-objective optimization study was carried out for a desiccant cooling system combined with solar and a GSHP • It was not feasible to ensure desired thermal comfort under high humidity conditions without the aid of GSHP. The payback period of the proposed system was 5.7 years
[102]	• A desiccant-based hybrid cooling system integrated with a GSHP was studied • Performance was evaluated in a humid climate in July for three cities in Italy and Iran • The combination of a GSHP with a DW ensured thermal comfort for more than 90% of the time for all three cities • Longer payback period and high installation cost are major barriers to market penetration at the consumer level • To overcome these barriers, district heating was considered

iii) DWs coupled with thermal energy storage and photovoltaics

Another way to improve the overall energy efficiency of the DW system is to combine it with photovoltaics and phase change material (PCM)–based thermal energy storage (TES). A schematic of such an integrated system is shown in **Figure 16**, as proposed by Ren et al. [103]. In this system, a photovoltaic thermal collector-solar air heater (PVT-SAH) provides the hot air for the regeneration process, and the PCM-TES unit acts as the thermal energy reservoir to fill the mismatch when the PVT-SAH unit cannot provide sufficient heat for regeneration. An auxiliary electric heater can also be used as a backup, which can be powered by the electrical energy generated by the PVT. Process air is first dehumidified using the DW, which increases the air temperature by the release of enthalpy of adsorption, which can be recovered using a heat recovery unit. Then, the process air can be further cooled by an evaporative cooler before being supplied to

the considered space. The PCM-TES unit can be changed using the hot air from the PVT-SAH. The regeneration air can be directly supplied from the PVT-SAH unit, or it can be mixed with another hot air stream from the heat recovery unit with or without passing through the PCM-TES unit.

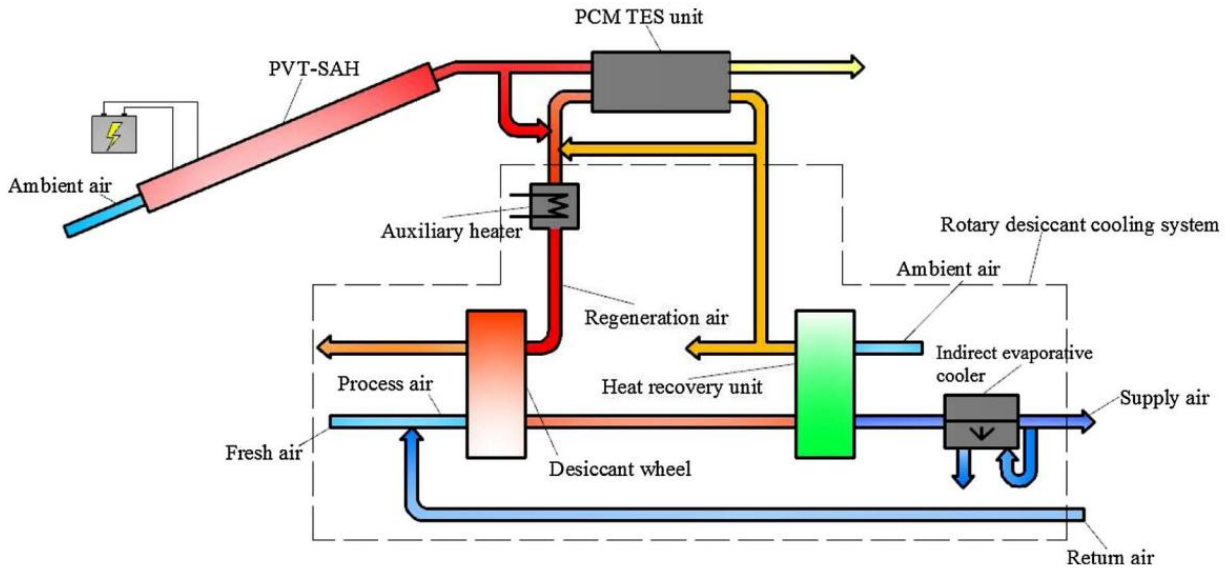

Figure 16. Schematic of a DW coupled with a photovoltaic thermal collector–solar air heater with TES [103].

Kabeel and Abdelgaied [104] numerically investigated the energy-saving potential of integrating solar and PCMs to a DW for three system configurations: Type A using an electrical heater, Type B using an electrical heater with a solar collector, and Type C using TES with a solar collector and electrical heater. The average energy-saving potential of Type B and Type C, respectively, were about 20.85% and 75.82% higher than that of Type A. Song and Sobhani [105] also investigated the performance of a solar- and PCM-assisted DW system, in which the PCM could deliver thermal energy for regeneration during the nighttime operation. The use of a PCM enhanced the thermal efficiency of the system, and a total COP of 0.404 was obtained. However, several key parameters need to be designed properly to obtain the best performance from a DW integrated with solar and TES, such as the amount and properties of the PCM; dimensions of the PCM storage tank, collector area, and solar thermal contribution; size of the DW; and so on [106].

4 DWs for VOC Mitigation

The two most common pathways for VOC removal from indoor air are photocatalytic oxidation and adsorption onto a suitable solid desiccant. However, considering an integrated HVAC system to simultaneously control humidity, VOCs, and CO_2, adsorption of VOCs using a DW stands out as a highly promising method. Moreover, the feasibility of regeneration below 100°C, simple design, and flexible wheel operation makes this method cost-effective and easy to be implemented in building HVAC systems. Several studies have investigated VOC removal performance using DWs for a wide range of adsorbents and VOC pollutants. **Figure 17** shows a typical experiment setup, which was used by Yamauchi et al. [107] to assess the performance of a DW as an air cleaner and dehumidifier.

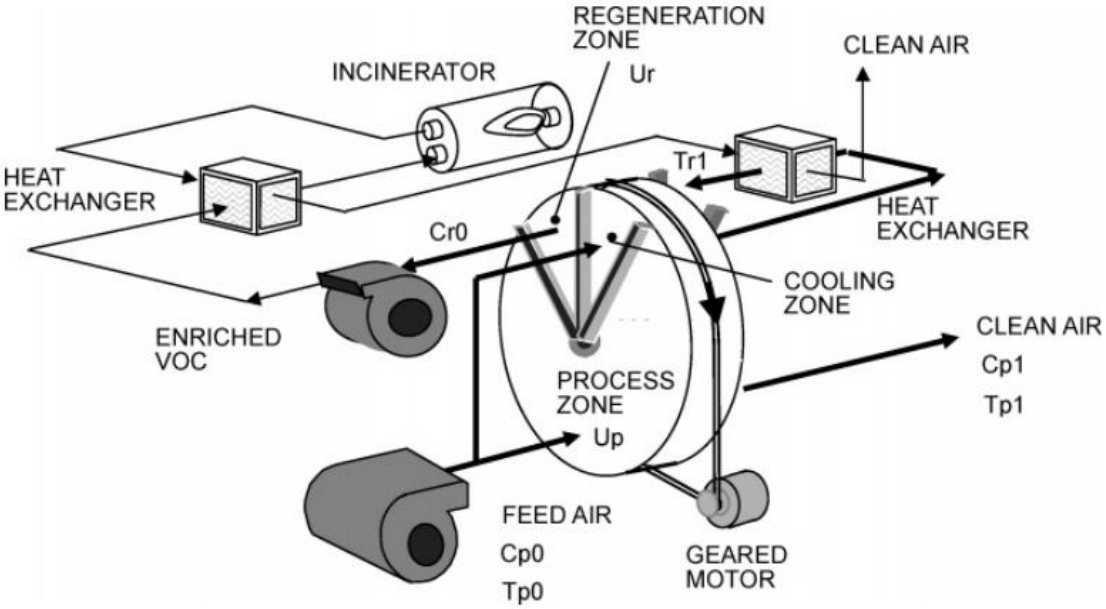

Figure 17. Schematic of a DW used to combinedly remove moisture and VOCs from process air [107].

4.1 Suitable Adsorbents for VOCs

Wang et al. [108] investigated three types of commonly used desiccants: activated carbon, silica gel, and zeolite 13X. The best adsorption performance of several VOCs including benzene, toluene, o-xylene, p-xylene, and m-xylene, characterized using the equilibrium isotherm, was found in the order of activated carbon, silica gel, and zeolite. Activated carbon exhibited the highest aromatics

uptake because of its nonpolar surface leading to a great affinity for the aromatics, large specific surface area, and pore volume. Zhu et al. [109] reviewed the VOC adsorption performance of different porous materials, including carbon-based materials, zeolites, MOFs, clays, silica, organic polymers, and composites. Tu et al. [110] reviewed the MOFs suitable for adsorbing aromatic-based VOCs, and Lai et al. [111] reviewed the MOFs suitable for capturing VOCs from Indoor pollution sources. Based on the above reviews, here we provide a summary **(Table 8)** of the MOFs those exhibited highest adsorption capacity of common VOCs.

Table 8: MOFs exhibiting highest adsorption capacity of common VOCs.

Adsorbate	**Adsorbent**	**Specific Surface Area (m^2/g)**	**Adsorption capacity (g/g)**	**Temperature (℃)**	**Source**
Toluene	UiO-67/GO	1052	0.876	25	Tu et al. [110]
	MIL-53 (Fe), Fe(OH)(BDC)	951	0.730	21	
	$(H_2O)_2(BDC)_3$	2728	2.115	21	
	CAU-1, $Al_4(OH)_2(OCH3)_4$	1209	0.528	25	
Benzene	MIL-101, $Cr_3O(OH)$	2925	1.17	25	Tu et al. [110]
	$(BDC)_3$	4293	0.829	25	
	MOF-5, $Zn_4O(BDC)_3$	3625	0.67	-	
	BTU-57, Co(PDP)	970	0.499	-	
Chlorobenzene	Styrene divinylbenzene	1020.7	0.389	30	Zhu et al. [109]
Formaldehyde	MIL-101(Cr)	-	0.10	Room	Lai et al. [111]
Xylene	Defect-rich UiO-67, $Zr_6O_4(OH)_4(BPDC)_6$	1767	0.382	25	Tu et al. [110]
	ZJU-620(Al), $Al_3O_3(HCOO)_3$(TMTA)	1347	0.33-0.34	25	
	ZU-61,Ni	1083	0.381-0.468	25	

Ethylbenzene, Styrene and Phenol	$(NbOF_5^{2-})BPY_2$				Tu et al. [110]
	ZJU-620(Al), $Al_3O_3(HCOO)_3$(TMTA)	1347	0.36	25	
	CNT@MIL-68(Al)	1407	0.34	-	

4.2 VOC Adsorption with DWs

Although many adsorbents are reported to adsorb VOCs and water vapor effectively, few studies have investigated applications using rotary adsorption for VOC and moisture control in buildings. Among these studies, the adsorbent used is typically silica gel because of its excellent moisture removal capacity, low regeneration temperature (<100°C), and easy access in the market. Few researchers used zeolite-based DW for VOC and moisture removal with a high regeneration temperature of 180°C. In general, commercially available DWs can provide efficient VOC removal capacity for air cleaning. **Table 9** summarizes the studies evaluating removal of VOCs from indoor air using DW.

Table 9. Studies evaluating removal of VOCs from indoor air using DWs

Ref.	Adsorbent	Sources/types of VOCs	Research highlights
[112]	Silica gel	Formaldehyde, acetone, ethanol, toluene, and 1,2-dichloroethane	• A clean-air heat pump (CAHP) was employed for VOC removal and the performance of CAHP was studied at different regeneration air temperatures (below 60°C) • At regeneration air temperatures above 40°C, total VOC removal efficiency was greater than 50%

			• A silica gel rotor showed a higher affinity to polar compounds (formaldehyde, acetone, and ethanol) than nonpolar compounds
[113]	Silica gel	Formaldehyde, acetone, ethanol, toluene, and 1,2-dichloroethane	• The influence of moisture content on the air cleaning performance of DWs in CAHPs was studied • Increasing the moisture content of the process air decreased the removal efficiency of VOCs by 5%–15% for water-soluble pollutants and by 20%–30% for non-water-soluble pollutants. • Thus, high moisture content adversely affected the VOC removal performance. To maintain high performance for both VOC removal and dehumidification simultaneously, optimizing regeneration temperature with automation was suggested
[114]	Silica gel	Flooring materials (old carpet and linoleum) and pure chemicals (acetone, ethanol, toluene, and 1,2-dichloroethane)	• The effect of regeneration temperature (25°C–70°C) on air cleaning in CAHPs was studied under low outdoor air supply rate for ventilation • An average single pass total VOC (TVOC) removal efficiency of 82.7% was achieved at a regeneration temperature of 60°C, and 96.7% at a regeneration temperature of 70°C
[115]	Silica gel	TVOC (source not mentioned)	• Combined TVOC and humidity removal capacity was studied under moderate temperature and humidity conditions and Shanghai summer (37°C, 65% RH) conditions • The TVOC removal effectiveness reached 80% at 100°C regeneration temperature under

			Shanghai summer conditions. Regeneration temperature above 100°C was recommended
[116]	Silica gel	Toluene and n-hexane	• Removal efficiency at low concentration (50–150 ppb) for indoor air-conditioning application was studied • At such low concentration, changing operating parameters (e.g., inlet TVOC concentration, inlet stream temperature, stream humidity ratio, and wheel rotation speed) had negligible influence on the TVOC removal performance.
[117]	Silica gel	Human subjects, flooring materials, formaldehyde, ethanol, toluene, and 1,2-dichloroethane	• High TVOC removal effectiveness (> 94%) was achieved for regeneration temperatures between 60°C–70°C • Using a regenerative DW in the ventilation system was found to be an efficient means for the removal of indoor VOCs
[107]	Hydrophobic zeolite with high Si/Al ratio	Acetone, isopropyl alcohol (IPA), methyl ethyl ketone (MEK), and toluene.	• The influence of VOC concentration in feed, process to regeneration airflow rate ratio, moisture content in air, and regeneration temperature were studied • Removal efficiency decreased with increasing concentration, flow rate ratio, and humidity • Removal efficiency reached its maximum at a regeneration temperature of 180°C • Optimum operating condition and rotation speed were suggested for maximum efficiency

Recently, more studies have reported the VOC adsorption performance of silica gel and zeolite, but limited studies examined the adsorption mechanisms. In general, silicate materials

exhibit more affinity toward the polar VOCs than nonpolar VOCs [118]. Silica gel has a fast adsorption speed and high adsorption capacity, in addition to its merit of excellent hydro-thermal, chemical and mechanical stability; high surface area; and numerous choices for functional groups [109]. Additionally, silica gel's adsorption capability is mainly influenced by the geometric barrier effect, and its adsorption capacity decreases as geometric barriers increase [108]. However, because of the hydrophilic surface of silica gel, it tends to exhibit limited adsorption efficiency when exposed to high humidity conditions.

For zeolite, adsorption of VOCs is also induced by polarity [108]. The molecular weight of VOCs causes an increasing adsorption capacity with larger molecular weights. The Si content of zeolites relates to their water resistance and can be customized during the synthesis process. Zeolite also has an adjustable specific surface and pore structure, and it is a very promising adsorbent. However, the process of synthesizing specific zeolites is complex and time-consuming [119].

4.3 Influence of Operating Conditions on VOC Removal

Wolfrum et al. [116] studied the influence of process air relative humidity (RH) on VOC removal (toluene and n-hexane) using a silicate-based DW. They reported a higher transfer rate for toluene compared to n-hexane, potentially due to the higher relative volatility of n-hexane. Additionally, they found that at 40% RH, there was no significant change in VOC removal performance when the inlet concentration varied between 60-150 ppb. However, as the inlet RH increased, a decrease in VOC removal efficiency was observed. Ge et al. [120] also reported that the total VOC (TVOC) removal capacity decreases with increasing RH **(Figure 18a)**. This is likely due to a reduction in the adsorption capacity of the wheel, as water vapor competes with VOCs for adsorption sites.

The TVOC removal efficiency is defined as the difference in VOC concentrations between the process air inlet and outlet divided by the inlet concentration. As shown in **Figure 18b,** the TVOC removal efficiency is also affected by the flowrate and concentration of TVOC in the inlet air stream. As flow rate increased, the wheel's removal capacity decreased as well. However, at very low concentrations, the removal capacity remained nearly constant regardless of flow rate, likely because the silica gel was far from saturation and still had sufficient capacity to remove the contaminants. Furthermore, the removal capacity decreased as the inlet TVOC concentration increased, potentially due to saturation of the desiccant wheel with a high amount of TVOC.

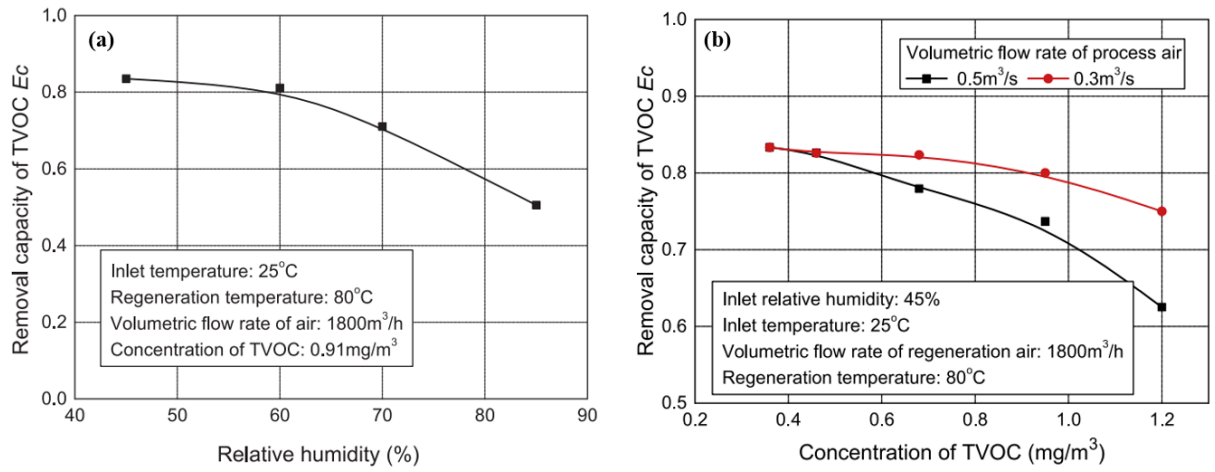

Figure 18. Influence of operating conditions on TVOC removal capacity DW. TVOC removal capacity as a function of (a) process air inlet relative humidity, and (b) process air inlet flow rates and concentration of TVOCs. (Source: Ge et al. [120]).

5 DWs for CO_2 Capture

5.1 Suitable Adsorbents for CO_2 Capture

CO_2 concentration in the atmosphere has increased by 123 ppm in 2016 from 280 ppm in the pre-industrial period [121]. To mitigate the rise of CO_2 concentration in the atmosphere and limit the global temperature rise below 2.0 ℃, 196 countries signed a treaty in Paris, on December 2015 [122]. Due to the increased concern about global temperature rise, direct air capture (DAC) of CO_2 from the ambient using solid desiccant materials has gained tremendous attention. Several authors [16, 123-125] have reviewed the CO_2 adsorption capacity of various solid desiccants including MOFs, silica-gel, zeolite, carbon and graphene-based adsorbents. **Table 10** lists the MOF, carbon nanotube, graphene and zeolite-based adsorbents those exhibited high CO_2 uptake capacity (≥0.60 mmol/g) at low operating pressure (0.10-0.20 atm). **Table 11** lists the MOF-based adsorbents those exhibited high CO_2 uptake capacity (≥18 mmol/g) at high operating pressure (24-50 bar).

Table 10. Adsorbents exhibited high CO_2 adsorption capacity (≥0.60 mmol/g) at low-pressure (0.10-0.20 atm) (Source: Raganati et al. [124])

Category	Adsorbent Name	Surface Area (m^2/g)	Temperature (K)	Pressure (atm)	Adsorption Capacity (mmol/g)
MOF-based	HKUST-1	680	298	0.15	1.14
	Ni/DOBDC	936	298	0.10	4.07
	Co/DOBDC	957	298	0.10	2.81
[1]CNT & Graphene-based	MWCNTs	-	293	0.20	0.84
	Graphene	477	273	0.15	0.70
Zeolite-based	13X	710	393	0.15	0.70
	NaX	534	323	0.20	0.60
	CaA	397	323	0.20	0.75
	CsY	842	333	0.10	0.86
	Naβ	570	273	0.15	2.30

[1]**CNT:** Carbon nanotube

Table 11. MOFs exhibited high CO_2 adsorption capacity (≥18 mmol/g) at high-pressure (24-50 bar) (Source: Liu et al. [123])

MOF Name	BET Surface Area (m^2/g)	Temperature (K)	Pressure (bar)	Adsorption Capacity (mol/kg)
MOF-200	4530	298	50	54.5
MOF-210	6240	298	50	54.5
NU-100	6143	298	40	46.4
MIL-101(Cr)	4230	304	50	40.0
MOF-205	4460	298	50	38.1
UMCM-1	4100	298	24	23.5
MOF-5	2833	298	35	21.7
IRMOF-6	2516	298	35	19.5
IRMOF-3	2160	298	35	18.7

5.2 CO_2 Capture with DWs and Other Rotating Beds

Various types of bed configurations have been explored for adsorption-based CO_2 capture and removal, including fixed [126], fluidized bed [127], and rotary bed [128]. The schematics of CO_2 adsorption beds used by Gupta et al. [129], Herriaz et al. [130], and Gao et al. [131] are shown in **Figure 19a–c,** respectively. The figure shows that the beds for CO_2 capture can be either a DW **(Figure 19a and b)**, or it can be a different configuration, such as packing under rotation **(Figure 19c)**. Nevertheless, rotary adsorption configurations have gained increasing interest in recent years because of their continuous operation, compact design, and suitability to be integrated into the ventilation systems of buildings. Rotary adsorption beds typically use structured adsorbents in the form of adsorbent sheets (laminate) or monoliths in the rotary wheel [132]. Unlike in the case of dehumidification, where the DW is divided into two segments (process and regeneration), in the case of CO_2 adsorption, it can be divided in up to four segments for adsorption, desorption, cooling, and heating **(Figure 19a)**. **Table 12** summarizes the studies on rotating beds for CO_2 capture. To be noted that these studies mainly investigated the potential of rotating beds for direct air capture of CO_2. However, the outcomes and insights of these studies can also be used for CO_2 capture for indoor air quality management.

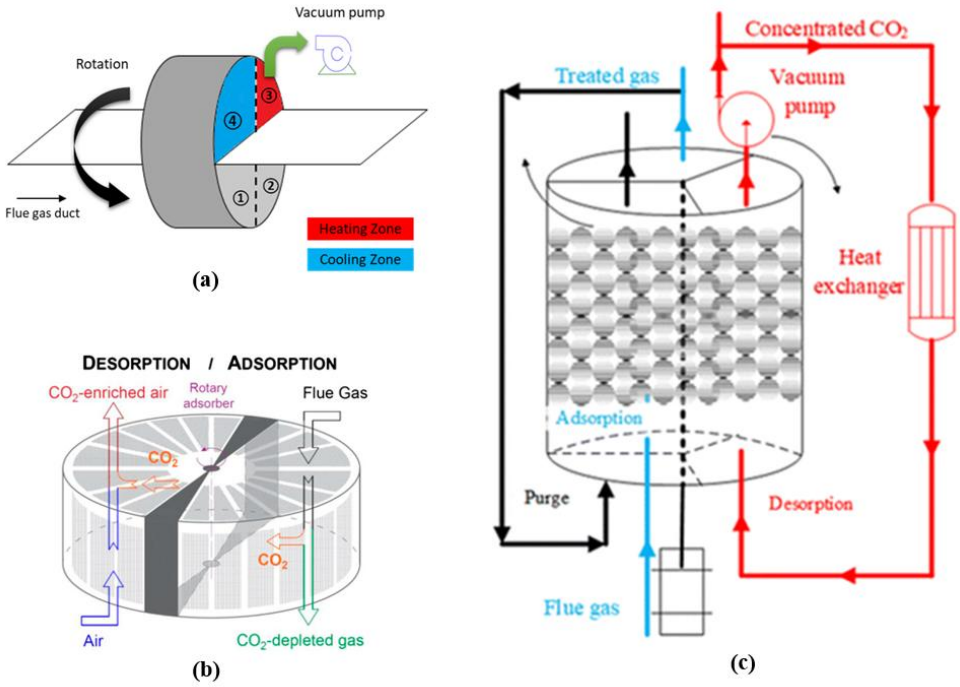

Figure 19. Schematic diagrams of rotating bed adsorbers for CO_2 capture. Rotating bed studied by (a) Gupta et al. [129], (b) Herriaz et al. [130], and (c) Gao et al. [131].

Table 12. Studies evaluating the performance of rotating bed adsorber for CO_2 capture.

Ref.	Configuration and research highlights
Carbon Capture Technology [133]	• Structured MOF in the form of laminate was studied • The rotary contactor machines divided into three sections for adsorption, desorption, and cooling • The process was a rapid cycle-temperature swing adsorption with direct steam regeneration • The process removed CO_2 from the air and flue gas
Rotary Adsorption Machine [134]	• The system used a rotating drum, or a set of drums lined with adsorbent material • Slowly rotating machines were integrated with a boiler air preheater into a rotary adsorber • The system withstood temperature and pressure fluctuations
Tang et al. (2022) [15]	• The sorbents were activated carbon, zeolite 13X, and Mg-MOF-74 • The cyclic adsorption-desorption process took place by rotation of the rotor in the adsorption and desorption sectors • A heat pump was used to heat the air for the desorption and cool the air for the adsorption
Herraiz et al. (2020) [130]	• A system was proposed for selective recycling of CO_2 present in the flue gas from a combined cycle gas turbine power plant • The rotary wheel under this study was divided into two sections that were periodically exposed to the flue gas and the ambient air streams in reverse directions • Activated carbon and zeolite 13X was employed as the desiccants and their regeneration was tested at near-ambient temperature and pressure • The authors proposed a model for rotary adsorber that can be used to determine the minimum amount and desired thermophysical properties of the desiccant; the dimensions of the wheel rotor; and predict the heat and mass transfer performance of the rotary adsorber

Gao et al. (2020) [131]	• The temperature vacuum swing adsorption process was employed in a rotary reactor. The height of the reactor column was divided into three segments for adsorption, desorption, and purging. • A treated gas was used to purge the reactor for the next adsorption • The authors evaluated the process via mathematical modeling
Gupta & Ghosh (2015) [129]	• Disc-shaped adsorbent sheets were mounted on a rotating structure parallel to each other with a gap between them • The adsorbent bed was divided into four equal sections with two cooling zones and two heating zones • A rotary adsorption bed could be added to the existing flue gas outlet duct of the power plant

5.3 Influence of Humidity on CO_2 Uptake

The existing literature [135, 136] reports that when the water molecules are present with CO_2 molecules, the CO_2 uptake capacity of solid adsorbents become lower due to the preferential adsorption of water vapor over CO_2. Liu et al. [135] studied the competitive adsorption between H_2O and CO_2 using two distinct MOFs (HKUST-1 and Ni/DOBDC) and compared the results with two different variations of Zeolite (5A and NaX). Their results showed that at high water loadings, both HKUST-1 and Ni/DOBDC MOFs preferentially adsorbed H_2O over CO_2. However, the CO_2 uptake capacity of zeolite adsorbents reduced more drastically than HKUST-1 and Ni/DOBDC at high water loading. Thus, the MOFs exhibited relatively higher CO_2 uptake capacity in the presence of H_2O that those of conventional zeolites. In another study Liu et al. [136] reported that Ni/DOBDC could maintain its CO_2 uptake capacity after steam conditioning, whereas CO_2 uptake capacity of Mg/DOBDC became nearly half after steam conditioning, indicating the poor stability of Mg/DOBDC in the presence of water vapor. Kolle et al. [16] reviewed the studies investigating humidity effect on CO_2 adsorption and summarized the data of CO_2 uptake capacity at dry condition and humid condition for a large number of MOFs, zeolites, polyamine impregnated adsorbents. **Table 13** provides a comparison of CO_2 uptake capacity of several MOFs in dry and humid conditions. From the table it can be seen that CO_2 uptake capacity could be reduced by as

much as 84% for Mg_2(dobdc) in the presence of water vapor. Hence, removing water vapor from the process air stream is crucial to maintain the high uptake capacity of CO_2.

Table 13. Humidity effect on CO_2 Adsorption (Source: Kolle et al. [16])

Adsorbent	Ref.	Pressure (atm)	Temperature (℃)	RH (%)	CO_2 uptake (mmol/g)		Uptake reduced (%)
					Dry	Humid	
Mg_2(dobdc)	Datta et al. (2015)	0.10	25	90	3.94	1.39	64.72
	Kumar at al. (2015)	0.15	30	100	5.34	1.54	71.16
	Kizzie et al. (2011)	0.17	25	70	5.36	0.85	84.14
	Kumar at al. (2015)	1.00	30	100	5.68	2.28	59.86
Co_2(dobdc)	Kizzie et al. (2011)	0.17	25	70	3.03	2.59	14.52
Zn_2(dobdc)	Kizzie et al. (2011)	0.17	25	70	1.65	0.36	78.18
Ni_2(dobdc)	Datta et al. (2015)	0.10	25	90	2.38	1.86	21.85
HKUST-1	Kumar at al. (2015)	0.15	30	100	1.59	0.29	81.76
MIL-101(Cr)	Kizzie et al. (2011)	0.50	30	50	2.44	1.37	43.85
UiO-66	Liang et al. (2009)	0.15	30	75	0.72	0.19	73.61

5.4 Energy Consumption for CO_2 Capture

Although CO_2 capture from ambient using porous solids is promising, but significant amount of energy input is needed in the form of heat regenerate the solid adsorbent and fan power to facilitate the flow of ambient air over the adsorbing bed. To reduce the energy input for fan power, recently, Kashkouli et al. [137] and An et al. [138] have investigated the possibility of integrating CO_2 capture device with existing building roof top heating ventilation and air-conditioning equipment. **Figure A2** in the appendix section shows the photograph of an integrated CO_2 capture device with building roof top unit. **Table 14** and **Table 15** provide the data of energy consumption for CO_2 capture from air using various solid adsorbents as reviewed by Raganati et al. [124] and An et al., [139] respectively. **Table 16** provides the data on regeneration temperature of solid desiccants for CO_2 capture as reported by several companies.

Table 14. Data on energy consumption for CO_2 capture using various solid adsorbents as reviewed by Raganati et al. [124].

Adsorbent	Regeneration Method	Energy Consumption (MJ/kg_{CO2})	Regeneration Strategy
NaUSY zeolite	TSA	3.40-4.5	Direct: hot product gas purge
13X zeolite	TSA	3.23	Indirect+N_2 purge
13X zeolite	TSA	2.21	Indirect
Carbon honeycomb monoliths	TSA	3.59	Indirect+ steam purge
Amine-functionalized	TSA	2.80	Indirect+vacuum+CO_2 purge
13X zeolite-activated carbon	VPSA	2.44	Two stages
13X zeolite	VPSA	2.64	Two stages
Activated Carbon	VPSA	3.61	Two stages
13X zeolite	VTSA	3.22	Two stages

TSA: Temperature Swing Adsorption; **VPSA:** Vacuum Pressure Swing Adsorption; **VTSA:** Vacuum Temperature Swing Adsorption.

Table 15. Data on energy consumption for CO_2 capture using various solid adsorbents as reviewed by An et al. [139].

Adsorbent	Regeneration Method	Heat Source	Energy Consumption (MJ/kg_{CO2})
MIL-101	-	-	1.83
$MmenMg_2$	-	-	1.18
Amine based Adsorbents (Deutz, 2021)	-	Heat Pump	2.03
Amine based Adsorbents (Deutz, 2021)	-	Waste Heat	1.12
Amine based Adsorbents (Elfving, 2021)	TVSA, 60 ℃	-	0.54
Amine based Adsorbents	TVSA, 100 ℃	-	1.51

(Elfving, 2021)			
Amine based Adsorbents (Sabatino, 2022)	-	-	18.75

Table 16. Regeneration temperature range for CO_2 capture using solid desiccant as reported by several companies (Source: Fasihi et al. [121])

Company	Country	Regeneration Temperature (℃)	Method
Climeworks	Switzerland	100	TSA
Global Thermostat	USA	85-95	
Antecy	Netherlands	800-100	
Hydrocell	Finland	70-80	
Skytree	`Netherlands	Moisturizing 80-90	MSA

TSA: Temperature Swing Adsorption; **MSA:** Moisture Swing Adsorption

5.5 Cost of CO_2 Capture

Estimating the cost of CO_2 capture is important for commercialization of the DAC technology. Recently, Kashkouli et al. [137] have conducted the techno-economic analysis (TEA) of a CO_2 capture technology integrated with a roof-top makeup air unit (MAU), utilizing triethylenetetramine (TETA)-modified polyacrylonitrile (PAN) fibers (PAN-TETA) as the adsorbent. A schematic of their MAU-CO_2 unit with PAN-TETA adsorbent is shown in **Figure A3** in the appendix section. The authors estimated the levelized cost per ton CO_2 captured (LCOC). LCOC is the sum of the levelized capital cost for MAU-CO_2 unit development, energy costs, transportation costs, and material regeneration costs. Assuming the operational lifetime of the MAU-CO_2 unit as 10 years, the sorbent production had the largest share of the total cost (85 %). Based on the TEA results of Kashkouli et al., identifying the low-cost adsorbents is the key to reduce the cost of CO_2 capture. Zentou et al. [125] have reported several low cost MOFs and zeolites for CO_2 capture with price range 32 – 200 USD/ton_{CO2} as listed in **Table 17**. Liu et al. [123] also provided data on the cost of raw materials (USD/kg) to produce some MOFs suitable for CO_2 capture as listed in **Table 18**.

Table 17. Low-cost MOF and other adsorbents for CO_2 capture from air and post-combustion. (Exchange rate: 1 Euro=1.09 USD, on 19.11.2023) (Source: as summarized by Zentou et al. [125])

Adsorbent Name	Method	Cost (USD/ton_{CO2})	CO_2 Source
MIL-101(Cr), PEI-800	TVSA (5 steps)	95-160	DAC
Mmen8Mg2(dobpdc)	TVSA (5 steps)	75-200	
TRI-PE-MCM-41	TSA(4 steps)	94.3-113.1	
MIL-101(Cr)	TSA(4 steps)	87	
Mg2(dobpdc)	TSA(4 steps)	88	
13X Zeolite (Hasan et al.)	PSA (4 steps)	82	Post-combustion
13X Zeolite (Hasan et al.)	VSA (4 steps)	64	
13X Zeolite (Leperi et al.)	PVSA (4 steps)	32.1	
Ni-MOF-74	PVSA (4 steps)	39.8	
MOF (Peh et al.)	PSA (4 steps)	91	

TVSA: Temperature Vacuum Swing Adsorption, **TSA:** Temperature Swing Adsorption, **PSA:** Pressure Swing Adsorption, **VSA:** Vacuum Swing Adsorption, **PVSA:** Pressure Vacuum Swing Adsorption, **DAC:** Direct Air Capture

Table 18. [1]Cost of raw materials to produce some MOFs (suitable for direct air capture of CO_2) and silica gel (Source: Liu et al. [123])

Adsorbent	Cost (USD/kg)
HKUST-1	20.08
MOF-5 (IRMOF-1)	2.93
Zn-MOF-74	1.90
Ni-MOF-74	6.48
Co-MOF-74	13.33
Mg-MOF-74	1.19
MIL-100	15.64
MIL-101	4.57
Silica gel	1.00

[1]Costs were based on purchase of one metric ton or greater quantity and data were published in 2012.

5.6 Regional Effect on Energy and Cost of CO_2 Capture

As discussed in the previous two sections, energy consumption and cost are the two crucial parameters for the commercialization and market penetration of CO_2 capture technology. However, as the CO_2 uptake capacity of solid adsorbents is dependent on the temperature and ambient relative humidity, the energy consumption and cost will also vary according to the climate conditions. Sendi et al. [140] have investigated the influence of different climatic conditions on the energy consumption and cost of CO_2 capture as summarized in **Table 19**. According to their findings, cold (<18 ℃) and humid (RH>65%) climate (e.g., UK, Europe, East Asia, Southern Australia and New Zealand) requires highest energy consumption, and hot (>18 ℃) and humid (RH>65%) requires the highest cost (e.g., Central and South America, Africa, South India and Southeast Asia).

Table 19. Regional effect on energy consumption and cost (Sendi et al.)

Climate Conditions	**Example Regions**	**Energy Required (MWh_{el}/ton_{CO2})**	**[1]Cost (US \$/ ton_{CO2})**
Cold (<18 ℃) and dry (RH<65%)	New Mexico, Wyoming, Central Asia	1.50-1.97 (mean: 1.76)	324-469 (mean: 365)
Cold (<18 ℃) and humid (RH>65%)	UK, Europe, East Asia, Southern Australia and New Zealand	1.81-2.56 (mean: 2.15)	320-525 (mean: 388)
Hot (>18 ℃) and dry (RH<65%)	West Texas, Sahara Desert, Middle East, Australia	1.45-1.94 (mean: 1.64)	327-499 (mean: 420)
Hot (>18 ℃) and humid (RH>65%)	Central and South America, Africa, South India and Southeast Asia	1.79-2.47 (mean: 2.11)	337-540 (mean: 462)

[1]Assuming cost of electricity US \$50/MWh, $_{el}$: electricity

6 Research Gaps and Future Research Directions

Based on the review of literature presented in this article, several key research gaps are identified by the authors to further enhance the performance of DWs for moisture removal, VOC and CO_2 adsorption, as discussed below.

6.1 Dehumidification: Research Gaps from the Perspective of Material Performance Improvement

i) High cost and mass production of MOF: Currently, superior MOFs for dehumidification application such as MIL-101(Cr) are synthesized at high temperature (>200 ^oC) and for prolonged periods (> 12 hr) [141], leading to a high cost of production. This also acts as barrier for mass production and market penetration of MOF-based DWs. Sibnath et al. [142] proposed the method of synthesizing Al-Fum at a 70°C solution temperature without using hazardous chemicals such as dimethylformamide. Such approaches should be extended for other potential MOFs for dehumidification application.

ii) Binder and pore blockage: At present, polymer binders are used to coat desiccant materials on the solid substrates used in DW using dip coating technique. While binders block the pore openings and reduces adsorbent loading, dip coating is not the most effective method to obtain an uniform coating thickness. In-situ synthesis can overcome these limitations by directly growing the MOF crystals on the substrate. Yang et al. [143] introduced a binder-free in situ synthesis of aluminum-based MOFs on an aluminum substrate, that exhibited high water absorption capacity of 192.5 g/m^2, the highest among reported desiccant-coated metal structures. Such approach should also be utilized in fabrication of DWs their performance.

iii) Composite and functionalized MOFs: MOFs possess high specific areas and pore volumes, however their low atomic density prevents them from providing sufficient dispersive forces to bind small molecules [144, 145]. Thus, new strategies were explored to improve atomic density of MOFs by preparing their composites, such as MOFs functionalized with graphene [146], graphite oxide [147, 148], carbon nanotubes [149], activated carbon [150], zeolite [151], and lithium chloride [152]. At present no literature demonstrates the performance of DWs with composite and functionalized MOFs due to the complexity of mass production and high cost. This

gap should be addressed in the future as DWs with composite and functionalized MOFs are expected to exhibit enhanced performance.

iv) Step-shape isotherm with controllable step location: A step-shape isotherm with controllable step locations at different humidity ranges would be more suitable for enhancing the dehumidification performance under various outdoor RH conditions. A recent study [153] showed that the step location of a diamine-appended MOF could be shifted toward high pressure at high temperatures by functionalizing it with various metal ions for CO_2 adsorption. However, demonstration of such control over the step-location of the isotherm for a MOF–water pair has not been reported. Thus, more research is needed in this direction for next-generation desiccant material development.

v) Stability under cyclic operation: The stability of water adsorption–desorption capacity under cyclic operation is another crucial parameter for practical dehumidification operation with DW. Han and Chakraborty [154] studied the cyclic stability of water vapor adsorption–desorption for parent MIL-53(Al) and its functionalized, protonated, and ligand-extended versions. The cyclic operation was carried out for over 150 cycles from adsorption (30°C and relative pressure of 0.9) to desorption (60°C and relative pressure of 0.1). The typical results of the cyclic stability tests for parent MIL-53(Al) and NH_2-functionalized MIL-53(Al) showed no decrease in adsorption capacity under long cyclic operation. Such studies also need to be extended for other potential MOFs and suitable adsorbents for dehumidification application.

vi) Topology of pore structure: The topology of pore structure (e.g., pore size, pore length, tortuosity, connectivity, number of pores) strongly influences the effective diffusivity of water vapor transport within the desiccant materials. For instance, for a mesoporous silica gel comprising macropores and micropores, using a cubic pore network model, Yu et al. [35] showed that increasing connectivity between pores resulted in improved diffusivity by reducing tortuosity and increasing porosity. The development of desiccant materials with tailored topology and structure may significantly improve the dehumidification capability of DWs. However, studies concerning optimizing parameters of the pore network of desiccant materials are scarce. This is another largely unexplored area that needs attention.

6.2 Research Gaps from the Perspective of Device Performance Improvement

i) Pressure drop: One key challenge in using DWs for dehumidification is the high pressure drop across the wheel because of the complex honeycomb structure. Shamim et al. [44] showed that the pressure drop of a conventional DW could be 38.5 times higher than that of a multilayer fixed-bed dehumidifier. Such a high pressure drop increases electricity consumption of the fan. However, this negative aspect of DWs is largely overlooked in the current literature. More simple and innovative structures should be proposed to reduce the pressure drop across the DW.

ii) Isothermal dehumidification: Isothermal dehumidification is key to enhancing the water vapor uptake capacity and reducing the cooling load after dehumidification. Few strategies for internal cooling of DWs have been proposed as shown earlier in **Figure 7,** but these strategies proved to be inadequate to achieve ideal isothermal dehumidification. However, staged cooling could do similar work as internal cooling, but the system size becomes bulky, and the cost increases by using multiple wheels. Therefore, achieving isothermal dehumidification with innovative designs of internal cooling and enhancing heat transfer is another key research gap that needs to be addressed for DWs.

iii) Waste recovery for regeneration: Heat input for regeneration, $\dot{Q}_{reg}$ is a key parameter that determines the overall performance of desiccant-based air-conditioning system. Shamim et al. [155] studied the influence of RH percentage in regeneration air on the moisture desorption capacity of a distinct mesoporous silica gel and showed that when the RH percentage in ambient air was high, larger heat input was necessary. To compensate for the additional heat demand under high ambient RH, recovery and re-utilization of waste heat can be a great option. Recently, waste heat recovery from data center cooling system [156, 157] has been receiving increased attention. Although the current literature report the utilization of waste heat for desiccant regeneration in DWs [158], this area is still largely unexplored.

6.3 Research Gaps in the Context of VOC Removal and CO_2 Capture

- The typical concentrations of VOCs and CO_2 are very low in indoor environments other than in industrial atmospheres. Most studies investigate removal efficiency at high

concentrations. Removal efficiency for indoor environments needs to be studied more exhaustively.

- The adsorption of VOCs and CO_2 is adversely affected by the presence of high moisture content in the process air. Therefore, three separate DWs need to be designed for adsorption of each component (i.e., water vapor, VOC and CO_2) to avoid competitive adsorption. The operating parameters (e.g., wheel rotation, regeneration temperature, process to regeneration airflow rate) should also be optimized for each DWs. Advanced and automated control systems need to be designed as well to optimize operating conditions for multiple DWs. To the best of authors' knowledge, no such study is reported yet investigating optimization of operating parameters for multiple DWs tailored for moisture removal, VOC and CO_2 capture.

- Majority of the studies in the literature uses DWs with silica gel for VOC adsorption and DWs with zeolite and activated carbon for CO_2 adsorption due to the low cost and ease of availability of these materials. No single adsorbent is appropriate for all cases. Hence, other adsorbents tailored for VOC and CO_2 adsorption should also be investigated with DWs.

- Fouling and pore blockage of adsorbents with particulate matters could be a real challenge to implement DW-based HVAC systems in highly polluted and dusty areas. Studies evaluating the presence of particulate matters in process air on VOC and CO_2 adsorption are scarce, which needs to be addressed. A recent study [159] has proved the feasibility of simultaneous cleaning of VOCs and fine particulate matter $PM_{2.5}$ using an electret filtration media . Such approaches can be extended for rotating DW systems, as well.

7 Conclusion

In summary, great potential exists to design an integrated, compact, low-cost, and energy-efficient HVAC system for the built environment using DWs capable of simultaneously adsorbing moisture, VOCs, and CO_2, thus provide thermal comfort and maintain high IAQ at the same time. To achieve

this goal, improvements should be aimed toward DW design and suitable adsorbent development. Finally, the following key conclusions can be drawn from the discussion presented in this article:

- Although there are several articles discussing DW performance for moisture removal available, studies addressing DW technology for VOC and CO_2 capture are still limited in the open literaure. Also, most studies on VOC capture and CO_2 removal with DW uses conventional silica-gel or zeolite as the adsorbent due to the low cost and availability of these materials.
- The key development goals from the DW device design perspective should be achieving isothermal adsorption, reducing pressure drop, integrating with waste heat recovery, and enhancing energy recovery of DWs.
- For suitable porous adsorbent development, key challenges are lowering the regeneration temperature, in-situ synthesis of adsorbents, reducing cost and facilitating mass production of MOF.
- Improving topology of pore structure, cyclic performance of adsorbents under long-term operation, and developing a step-shape isotherm with controllable step locations should also be prioritized.
- Optimization of operating conditions of multiple DWs to be used for humidity, VOC and CO_2 removal is another key area that needs attention.
- Lastly, although direct air capture of CO_2 with DW is a promising option, high energy consumption and high cost of adsorbent materials are the major barriers for commercialization of this technology.

The authors expect that the insights provided this review will be of significant interest to researchers in the HVAC industry, encourage them to pursue research initiatives that address the challenges outlined in this article, and thereby positioning DW technology as a more attractive solution for energy-efficient -IAQ management in buildings.

Nomenclature

Symbol	Description	Unit
$\omega_{pa,in}$	Specific humidity in process air inlet	g/kg_{DA}

$\omega_{pa,out}$	Specific humidity in process air outlet	g/kg$_{DA}$
$\dot{m}_{pa}$	Mass flow rate of process air	Kg/s
$\dot{Q}_{reg}$	Regeneration heat input	KW
$\dot{Q}_c$	Cooling capacity	KW
h_{lat}	Enthalpy of moisture adsorption	KJ/mol
W_{reg}	Regeneration power	KW
DW	Desiccant wheel	-
VOC	Voltatile organic compounds	-
MOF	Metal organic frameworks	-
SG	Silica gel	-
MS	Molecular sieve	-

Subscripts

Symbol	**Description**
pa	Process air
C	Cooling
reg	Regeneration
lat	Latent

Acknowledgement

This study was funded by the US Department of Energy (DOE) Office of Energy Efficiency and Renewable Energy, Building Technologies Office (BTO). This manuscript has been authored by UT-Battelle, LLC, under contract DE-AC05-00OR22725 with the US Department of Energy (DOE). The US Government retains and the publisher, by accepting the article for publication, acknowledges that the US government retains a nonexclusive, paid-up, irrevocable, worldwide license to publish or reproduce the published form of this manuscript or allow others to do so, for the US government purposes. DOE will provide public access to these results of federally sponsored research in accordance with the DOE Public Access Plan (http://energy.gov/downloads/doe-public-access-plan)

Authors' contribution

JAS: Conceptualization, literature review, data analysis, original draft, and final revision; **XL:** Conceptualization, literature review and original draft, **EK:** conceptualization, writing, critical discussion, review and editing, **KL, MM, HJ and PIK:** conceptualization, writing, review and editing, **KN:** conceptualization, review of data, review - original draft, resource allocation and project management.

Declaration

The authors declare no known competing interest.

Appendix.

Table A1. List of frequently used keywords used for literature search either as a single word or as combination of different words

Adsorption	Volatile Organic Compounds	Humidity
Dehumidification	VOC Removal	Energy Consumption
Moisture Removal	CO_2 Capture	Techno Economic Analysis
Rotary Desiccant Wheel	Regeneration	Indoor Air Quality
Direct Air Capture	Temperature	Metal Organic Frameworks
Super Adsorbent Polymers	Thermoresponsive Hydrogels	Silica gel
Zeolite	Activated Carbon	Competitive Adsorption
Adsorption Mechanism	Adsorption Isotherm	Porous Media
[1]HVAC	[2]SSLC	Conventional Air-conditioning

[1]HVAC: Heating Ventilation and Air Conditioning; [2]SSLC: Separate Sensible and Latent Cooling

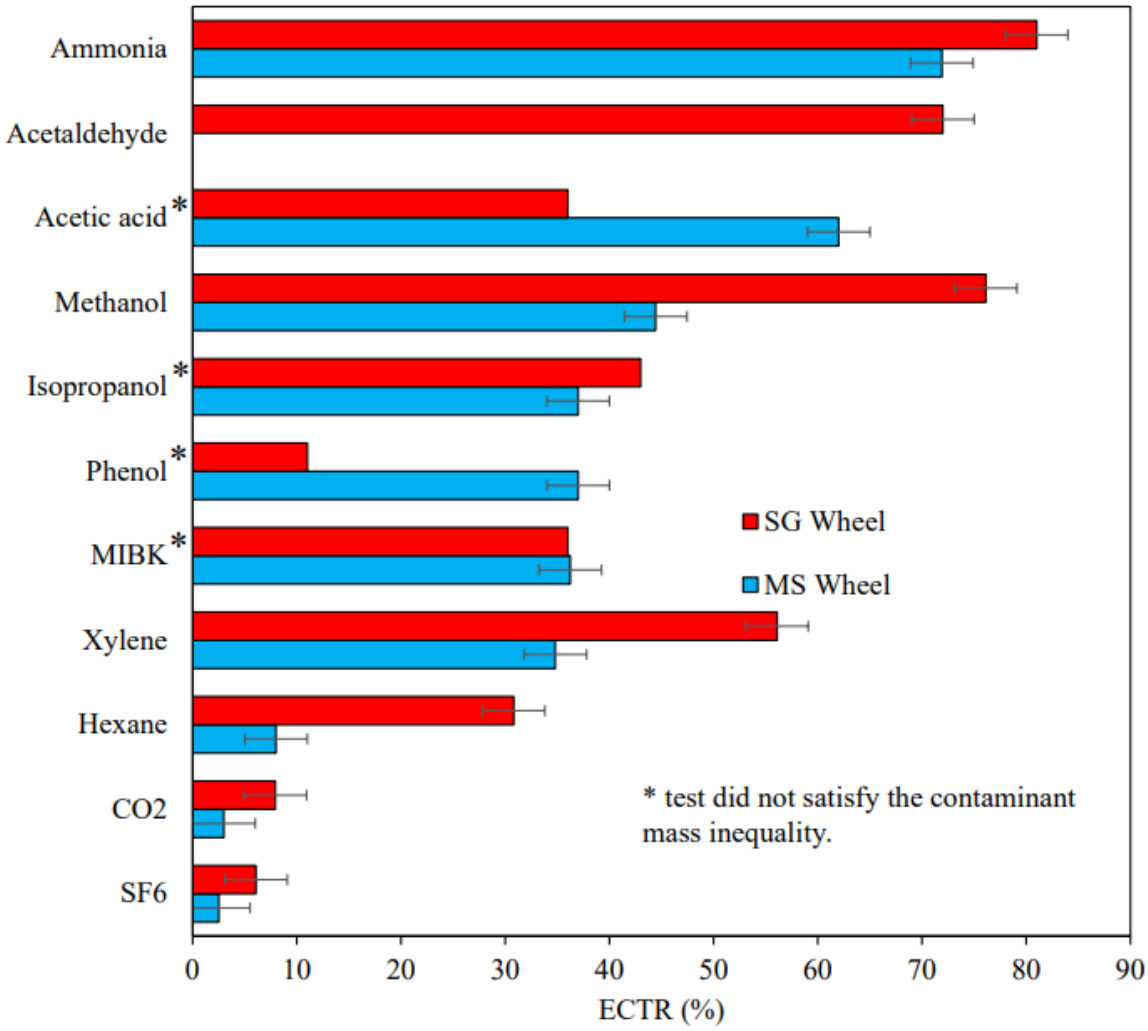

Figure A1. Exhaust contaminant transfer ratio (ECTR) of different gaseous contaminants for molecular sieve and silica gel coated wheels at room conditions. ECTR is defined as the difference in the concentration of gaseous contaminants between the supply air outlet and the supply air inlet, divided by the concentration difference of gaseous contaminants between the exhaust air inlet and the supply air inlet, and expressed as a percentage [18].

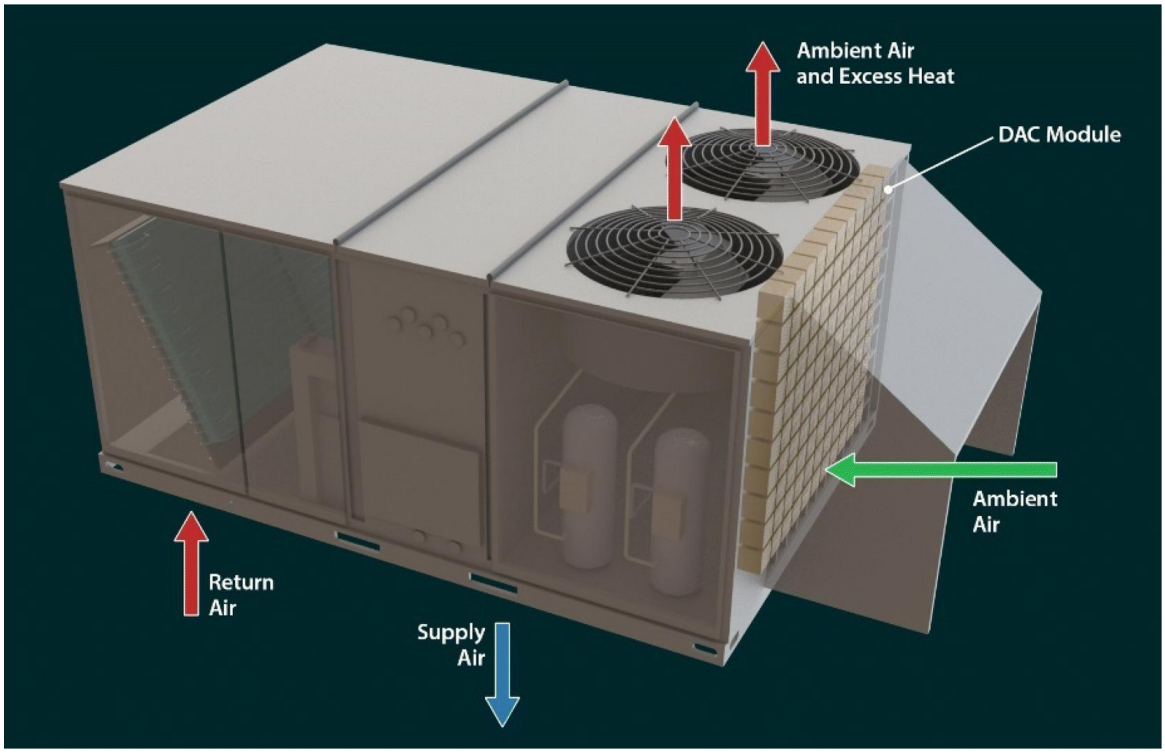

Figure A2. Schematic of direct air capture module integrated with a roof top air handling unit investigated by An et al. [138].

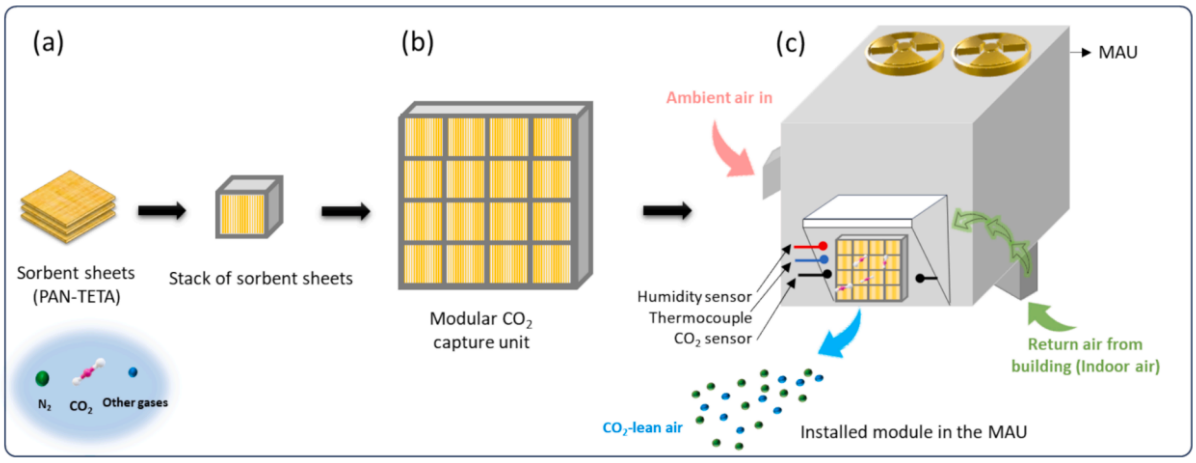

Fig. 3. A schematic representation of the (a) PAN-TETA sorbent sheets, (b) CO_2 capture unit, and (c) the coupled MAU-CO_2 capture module.

Figure A3. Schematic of triethylenetetramine (TETA)-modified polyacrylonitrile (PAN) fibers (PAN-TETA) CO_2 capture unit combined with a roof top makeup air unit (MAU) investigated by Kashkouli et al. [137].

References

[1] 2020 ASHRAE HANDBOOK: Heating, Ventilating, and Air-Conditioning, SYSTEMS AND EQUIPMENT, Inch-Pound Edition ed., ASHRAE, 1791 Tullie Circle, N.E., Atlanta, GA 30329, 2020.
[2] J. Woods, N. James, E. Kozubal, E. Bonnema, K. Brief, L. Voeller, J. Rivest, Humidity's impact on greenhouse gas emissions from air conditioning, Joule, 6(4) (2022) 726-741.
[3] A. Giampieri, Z. Ma, J. Ling-Chin, A.P. Roskilly, A.J. Smallbone, An overview of solutions for airborne viral transmission reduction related to HVAC systems including liquid desiccant air-scrubbing, Energy, 244 (2022) 122709.
[4] J.A. Shamim, W.-L. Hsu, S. Paul, L. Yu, H. Daiguji, A review of solid desiccant dehumidifiers: Current status and near-term development goals in the context of net zero energy buildings, Renewable and Sustainable Energy Reviews, 137 (2021) 110456.
[5] J.A. Shamim, W.-L. Hsu, H. Daiguji, Review of component designs for post-COVID-19 HVAC systems: possibilities and challenges, Heliyon, 8(3) (2022).
[6] Y. Chu, P. Xu, Y. Jia, M. Lin, C. Peng, Q. Dou, An adsorption-based CO2 treatment unit for ultra-low fresh air HVAC system using solid amine, Energy and Buildings, 247 (2021) 111148.
[7] P. Wolkoff, Indoor air humidity, air quality, and health–An overview, International journal of hygiene and environmental health, 221(3) (2018) 376-390.
[8] S. Sadrizadeh, R. Yao, F. Yuan, H. Awbi, W. Bahnfleth, Y. Bi, G. Cao, C. Croitoru, R. de Dear, F. Haghighat, Indoor air quality and health in schools: A critical review for developing the roadmap for the future school environment, Journal of Building Engineering, 57 (2022) 104908.
[9] L. Mølhave, G. Clausen, B. Berglund, J. De Ceaurriz, A. Kettrup, T. Lindvall, M. Maroni, A. Pickering, U. Risse, H. Rothweiler, Total volatile organic compounds (TVOC) in indoor air quality investigations, Indoor Air, 7(4) (1997) 225-240.
[10] D. Chen, G. Huebner, E. Bagkeris, M. Ucci, D. Mumovic, Effects of short-term exposure to moderate pure carbon dioxide levels on cognitive performance, health symptoms and perceived indoor environment quality, Building and Environment, 245 (2023) 110967.
[11] O. Seppänen, W. Fisk, M.J. Mendell, Association of ventilation rates and CO2 concentrations with health andother responses in commercial and institutional buildings, Indoor air, 9(4) (1999) 226-252.
[12] B. Chenari, J.D. Carrilho, M.G. Da Silva, Towards sustainable, energy-efficient and healthy ventilation strategies in buildings: A review, Renewable and Sustainable Energy Reviews, 59 (2016) 1426-1447.
[13] R. Shaughnessy, R. Sextro, What is an effective portable air cleaning device? A review, Journal of occupational and environmental hygiene, 3(4) (2006) 169-181.

[14] J. Nie, L. Fang, G. Zhang, Y. Sheng, X. Kong, Y. Zhang, B.W. Olesen, Theoretical study on volatile organic compound removal and energy performance of a novel heat pump assisted solid desiccant cooling system, Building and Environment, 85 (2015) 233-242.
[15] C. Tang, X. Gao, Y. Shao, L. Wang, K. Liu, R. Gao, D. Che, Investigation on the rotary regenerative adsorption wheel in a new strategy for CO2 enrichment in greenhouse, Applied Thermal Engineering, 205 (2022) 118043.
[16] J.M. Kolle, M. Fayaz, A. Sayari, Understanding the Effect of Water on CO2 Adsorption, Chemical Reviews, 121(13) (2021) 7280-7345.
[17] E. Hunter-Sellars, J.J. Tee, I.P. Parkin, D.R. Williams, Adsorption of volatile organic compounds by industrial porous materials: Impact of relative humidity, Microporous and Mesoporous Materials, 298 (2020) 110090.
[18] E.N. Krishnan, J. Soltan, C. Simonson, ASHRAE Research Project 1780: Test Method to Evaluate Cross-Contamination of Gaseous Contaminants within Total Energy Recovery Wheels, 2023.
[19] N. Asim, M.H. Amin, M. Alghoul, M. Badiei, M. Mohammad, S.S. Gasaymeh, N. Amin, K. Sopian, Key factors of desiccant-based cooling systems: Materials, Applied Thermal Engineering, 159 (2019) 113946.
[20] P. Vivekh, M. Kumja, D. Bui, K. Chua, Recent developments in solid desiccant coated heat exchangers–A review, Applied energy, 229 (2018) 778-803.
[21] T. Venegas, M. Qu, K. Nawaz, L. Wang, Critical review and future prospects for desiccant coated heat exchangers: Materials, design, and manufacturing, Renewable and Sustainable Energy Reviews, 151 (2021) 111531.
[22] X. Wu, T. Ge, Y. Dai, R. Wang, Review on substrate of solid desiccant dehumidification system, Renewable and Sustainable Energy Reviews, 82 (2018) 3236-3249.
[23] O.M. Zaki, R.H. Mohammed, O. Abdelaziz, Separate sensible and latent cooling technologies: A comprehensive review, Energy Conversion and Management, 256 (2022) 115380.
[24] D. Jani, M. Mishra, P.K. Sahoo, Solid desiccant air conditioning–A state of the art review, Renewable and Sustainable Energy Reviews, 60 (2016) 1451-1469.
[25] K.S. Rambhad, P.V. Walke, D. Tidke, Solid desiccant dehumidification and regeneration methods—A review, Renewable and Sustainable Energy Reviews, 59 (2016) 73-83.
[26] T.S. Ge, Y.J. Dai, R.Z. Wang, Review on solar powered rotary desiccant wheel cooling system, Renewable & Sustainable Energy Reviews, 39 (2014) 476-497.
[27] S. Tian, X. Su, Y. Geng, Review on heat pump coupled desiccant wheel dehumidification and air conditioning systems in buildings, Journal of Building Engineering, 54 (2022) 104655.

[28] M.M. Abd-Elhady, M.S. Salem, A.M. Hamed, El-Sharkawy, II, Solid desiccant-based dehumidification systems: A critical review on configurations, techniques, and current trends, International Journal of Refrigeration, 133 (2022) 337-352.
[29] X. Su, Y.N. Geng, L. Huang, S.G. Li, Q.B. Wang, Z.H. Xu, S.C. Tian, Review on dehumidification technology in low and extremely low humidity industrial environments, Energy, 302 (2024).
[30] M.A. Al-Ghouti, D.A. Da'ana, Guidelines for the use and interpretation of adsorption isotherm models: A review, Journal of Hazardous Materials, 393 (2020) 122383.
[31] M. Mozaffari Majd, V. Kordzadeh-Kermani, V. Ghalandari, A. Askari, M. Sillanpää, Adsorption isotherm models: A comprehensive and systematic review (2010−2020), Science of The Total Environment, 812 (2022) 151334.
[32] L. Yu, W.-L. Hsu, S. Fei, H. Daiguji, Water adsorption kinetics of silica based porous desiccants by volumetric method, International Journal of Heat and Mass Transfer, 202 (2023) 123738.
[33] A.A. Pesaran, A.F. Mills, Moisture transport in silica gel packed beds—I.Theoretical study, International Journal of Heat and Mass Transfer, 30(6) (1987) 1037-1049.
[34] Z. Li, S. Michiyuki, F. Takeshi, Experimental study on heat and mass transfer characteristics for a desiccant-coated fin-tube heat exchanger, International Journal of Heat and Mass Transfer, 89 (2015) 641-651.
[35] L. Yu, W.-L. Hsu, J.A. Shamim, H. Daiguji, Pore network modeling of a solid desiccant for dehumidification applications, International Journal of Heat and Mass Transfer, 186 (2022) 122456.
[36] A.A. Bezrukov, D.J. O'Hearn, V. Gascón-Pérez, S. Darwish, A. Kumar, S. Sanda, N. Kumar, K. Francis, M.J. Zaworotko, Metal-organic frameworks as regeneration optimized sorbents for atmospheric water harvesting, Cell Reports Physical Science, 4(2) (2023).
[37] R.H. Mohammed, E. Rashad, R. Huo, M. Su, L.C. Chow, Pore-size engineered nanoporous silica for efficient adsorption cooling and desalination cycle, npj Clean Water, 4(1) (2021) 38.
[38] D.D. Do, Asorption Analysis: Equilibria and Kinetics, Imperial College Press 1998.
[39] K. Kashiwagi, D. Suh, J. Hwang, W.-L. Hsu, H. Daiguji, Molecular simulations of water adsorption and transport in mesopores with varying hydrophilicity arrangements, Nanoscale, 10(24) (2018) 11657-11669.
[40] C. Schlumberger, M. Thommes, Characterization of Hierarchically Ordered Porous Materials by Physisorption and Mercury Porosimetry—A Tutorial Review, Advanced Materials Interfaces, 8(4) (2021) 2002181.
[41] P.W. Meyer, S. Cui, Y. Zeng, A. Aday, J. Woods, Engineered Polymer Architectures for Thermo-Responsive Desiccants in Dehumidification Applications, Advanced Energy Materials, 13(34) (2023) 2300990.

[42] N. Enteria, K. Mizutani, The role of the thermally activated desiccant cooling technologies in the issue of energy and environment, Renewable and Sustainable Energy Reviews, 15(4) (2011) 2095-2122.
[43] F.E. Nia, D. Van Paassen, M.H. Saidi, Modeling and simulation of desiccant wheel for air conditioning, Energy and buildings, 38(10) (2006) 1230-1239.
[44] J.A. Shamim, W.-L. Hsu, K. Kitaoka, S. Paul, H. Daiguji, Design and performance evaluation of a multilayer fixed-bed binder-free desiccant dehumidifier for hybrid air-conditioning systems: Part I– experimental, International Journal of Heat and Mass Transfer, 116 (2018) 1361-1369.
[45] W.-L. Hsu, S. Paul, J.A. Shamim, K. Kitaoka, H. Daiguji, Design and performance evaluation of a multilayer fixed-bed binder-free desiccant dehumidifier for hybrid air-conditioning systems: Part II– Theoretical analysis, International Journal of Heat and Mass Transfer, 116 (2018) 1370-1378.
[46] J.A. Shamim, S. Paul, W.-L. Hsu, K. Kitaoka, H. Daiguji, Theoretical analysis of transient heat and mass transfer during regeneration in multilayer fixed-bed binder-free desiccant dehumidifier: Model validation and parametric study, International Journal of Heat and Mass Transfer, 134 (2019) 1024-1040.
[47] K. Ando, A. Kodama, T. Hirose, M. Goto, H. Okano, Experimental study on a process design for adsorption desiccant cooling driven with a low-temperature heat, Adsorption, 11 (2005) 631-636.
[48] M. Goldsworthy, S. White, Design and performance of an internal heat exchange desiccant wheel, International Journal of Refrigeration, 39 (2014) 152-159.
[49] R. Narayanan, W. Saman, S. White, A non-adiabatic desiccant wheel: Modeling and experimental validation, Applied Thermal Engineering, 61(2) (2013) 178-185.
[50] C. Bongs, A. Morgenstern, Y. Lukito, H.-M. Henning, Advanced performance of an open desiccant cycle with internal evaporative cooling, Solar Energy, 104 (2014) 103-114.
[51] Y. Feng, Y. Dai, R. Wang, T. Ge, Insights into desiccant-based internally-cooled dehumidification using porous sorbents: From a modeling viewpoint, Applied Energy, 311 (2022) 118732.
[52] M. Jagirdar, P.S. Lee, J.T. Padding, Performance of an internally cooled and heated desiccant-coated heat and mass exchanger: Effectiveness criteria and design methodology, Applied Thermal Engineering, 188 (2021) 116593.
[53] L. Zhao, R. Wang, T. Ge, Desiccant coated heat exchanger and its applications, International Journal of Refrigeration, 130 (2021) 217-232.
[54] X. Zhou, R. Reece, Experimental investigation for a non-adiabatic desiccant wheel with a concentric structure at low regeneration temperatures, Energy Conversion and Management, 201 (2019) 112165.
[55] S.Z. Shahvari, J.D. Clark, Approaching theoretical maximum energy performance for desiccant dehumidification using staged and optimized metal-organic frameworks, Applied Energy, 331 (2023) 120421.

[56] X. Zheng, T. Ge, R. Wang, Recent progress on desiccant materials for solid desiccant cooling systems, Energy, 74 (2014) 280-294.
[57] M. Sultan, I.I. El-Sharkawy, T. Miyazaki, B.B. Saha, S. Koyama, An overview of solid desiccant dehumidification and air conditioning systems, Renewable and Sustainable Energy Reviews, 46 (2015) 16-29.
[58] A. Karmakar, V. Prabakaran, D. Zhao, K.J. Chua, A review of metal-organic frameworks (MOFs) as energy-efficient desiccants for adsorption driven heat-transformation applications, Applied energy, 269 (2020) 115070.
[59] J.A. Shamim, G. Auti, H. Kimura, S. Fei, W.-L. Hsu, H. Daiguji, A. Majumdar, Concept of a hybrid compression-adsorption heat pump cycle, Cell Reports Physical Science, 3(11) (2022).
[60] H. Kim, S. Yang, S.R. Rao, S. Narayanan, E.A. Kapustin, H. Furukawa, A.S. Umans, O.M. Yaghi, E.N. Wang, Water harvesting from air with metal-organic frameworks powered by natural sunlight, Science, 356(6336) (2017) 430-434.
[61] Q. Wang, D. Astruc, State of the art and prospects in metal–organic framework (MOF)-based and MOF-derived nanocatalysis, Chemical reviews, 120(2) (2019) 1438-1511.
[62] R. Freund, O. Zaremba, G. Arnauts, R. Ameloot, G. Skorupskii, M. Dincă, A. Bavykina, J. Gascon, A. Ejsmont, J. Goscianska, The current status of MOF and COF applications, Angewandte Chemie International Edition, 60(45) (2021) 23975-24001.
[63] A.E. Baumann, D.A. Burns, B. Liu, V.S. Thoi, Metal-organic framework functionalization and design strategies for advanced electrochemical energy storage devices, Communications Chemistry, 2(1) (2019) 86.
[64] H. Liu, S. Sundarrajan, G.V. Kumar, S. Ramakrishna, Review on polymer materials for solid desiccant cooling system, Macromolecular Materials and Engineering, 308(12) (2023) 2300176.
[65] S. Ashraf, M. Sultan, M. Bahrami, C. McCague, M.W. Shahzad, M. Amani, R.R. Shamshiri, H.M. Ali, Recent progress on water vapor adsorption equilibrium by metal-organic frameworks for heat transformation applications, International Communications in Heat and Mass Transfer, 124 (2021) 105242.
[66] A.-D. Raya, S. Mahmoud, E. Elsayed, P. Youssef, F. Al-Mousawi, Metal-organic framework materials for adsorption heat pumps, Energy, 190 (2020) 116356.
[67] A.N. Aziz, S. Mahmoud, R. Al-Dadah, M.A. Ismail, M.K. Al Mesfer, Numerical and experimental investigation of desiccant cooling system using metal organic framework materials, Applied Thermal Engineering, 215 (2022) 118940.

[68] Z. Liu, C. Cheng, J. Han, Z. Zhao, X. Qi, Experimental evaluation of the dehumidification performance of a metal organic framework desiccant wheel, International Journal of Refrigeration, 133 (2022) 157-164.
[69] M.H. Park, J.Y. Chung, S.H. Hong, J. Baek, M. Lee, D. Lee, Y. Kim, Performance characteristics of desiccant rotor using metal organic framework material, Applied Thermal Engineering, 223 (2023) 120066.
[70] S.Z. Shahvari, V.A. Kalkhorani, C.R. Wade, J.D. Clark, Benefits of metal–organic frameworks sorbents for sorbent wheels used in air conditioning systems, Applied Thermal Engineering, 210 (2022) 118407.
[71] S.Z. Shahvari, V.A. Kalkhorani, J.D. Clark, Performance evaluation of a metal organic frameworks based combined dehumidification and indirect evaporative cooling system in different climates, International Journal of Refrigeration, 140 (2022) 186-197.
[72] A. Mignon, N. De Belie, P. Dubruel, S. Van Vlierberghe, Superabsorbent polymers: A review on the characteristics and applications of synthetic, polysaccharide-based, semi-synthetic and 'smart'derivatives, European Polymer Journal, 117 (2019) 165-178.
[73] J. Lee, D.-Y. Lee, Sorption characteristics of a novel polymeric desiccant, International Journal of Refrigeration, 35(7) (2012) 1940-1949.
[74] T. Higashi, L. Zhang, M. Saikawa, M. Yamaguchi, C. Dang, E. Hihara, Theoretical and experimental studies on isothermal adsorption and desorption characteristics of a desiccant-coated heat exchanger, International Journal of Refrigeration, 84 (2017) 228-237.
[75] S.D. White, M. Goldsworthy, R. Reece, T. Spillmann, A. Gorur, D.-Y. Lee, Characterization of desiccant wheels with alternative materials at low regeneration temperatures, International Journal of Refrigeration, 34(8) (2011) 1786-1791.
[76] H. Kang, D.-Y. Lee, Experimental investigation and introduction of a similarity parameter for characterizing the heat and mass transfer in polymer desiccant wheels, Energy, 120 (2017) 705-717.
[77] C.-H. Chen, C.-Y. Hsu, C.-C. Chen, S.-L. Chen, Silica gel polymer composite desiccants for air conditioning systems, Energy and buildings, 101 (2015) 122-132.
[78] F. Zhao, X. Zhou, Y. Liu, Y. Shi, Y. Dai, G. Yu, Super moisture‐absorbent gels for all‐weather atmospheric water harvesting, Advanced Materials, 31(10) (2019) 1806446.
[79] J. He, H. Yu, L. Wang, J. Yang, Y. Zhang, W. Huang, C. Ouyang, Hygroscopic photothermal sorbents for atmospheric water harvesting: From preparation to applications, European Polymer Journal, (2023) 112582.

[80] P.W. Charles, Thermo-responsive Hydrogel Desiccant Material. UC San Diego. ProQuest ID: Charles_ucsd_0033M_16132. Merritt ID: ark:/13030/m547901w. Retrieved from https://escholarship.org/uc/item/5q19g3kv, (2016).
[81] Y. Zeng, J. Woods, S. Cui, The energy saving potential of thermo-responsive desiccants for air dehumidification, Energy Conversion and Management, 244 (2021) 114520.
[82] Y. Xue, Q. Li, R. Wang, T. Ge, Performance analysis of a rotary desiccant wheel using polymer material with high water uptake and low regeneration temperature, International Journal of Refrigeration, 158 (2024) 385-392.
[83] Y. Liu, Z. Liu, Z. Wang, W. Sun, F. Kong, Experimental evaluation of a hydrogel composite desiccant wheel for dehumidification with high water uptake and low regeneration temperature, Applied Thermal Engineering, 257 (2024) 124399.
[84] P.K. Kushwaha, A. Kumar, R. Choudhary, Effect of operating parameters of desiccant wheel on the performance of solar desiccant dehumidifier, Environmental Progress & Sustainable Energy, 43(5) (2024) e14361.
[85] K.K. Bhabhor, D.B. Jani, Performance analysis of desiccant dehumidifier with different channel geometry using CFD, Journal of Building Engineering, 44 (2021) 103021.
[86] S. Muthu, P. Talukdar, S. Jain, Effect of Regeneration Section Angle on the Performance of a Rotary Desiccant Wheel, Journal of Thermal Science and Engineering Applications, 8(1) (2015).
[87] G. Panaras, E. Mathioulakis, V. Belessiotis, N. Kyriakis, Experimental validation of a simplified approach for a desiccant wheel model, Energy and Buildings, 42(10) (2010) 1719-1725.
[88] J.D. Chung, D.-Y. Lee, Effect of desiccant isotherm on the performance of desiccant wheel, International Journal of Refrigeration, 32(4) (2009) 720-726.
[89] M. Hyeon Park, J. Yeob Chung, S. Ho Hong, J. Baek, M. Lee, D. Lee, Y. Kim, Performance characteristics of desiccant rotor using metal organic framework material, Applied Thermal Engineering, 223 (2023) 120066.
[90] The Future of Heat Pumps. https://www.iea.org/reports/the-future-of-heat-pumps (accessed 02/13/2025).
[91] J. Rosenow, D. Gibb, T. Nowak, R. Lowes, Heating up the global heat pump market, Nature Energy, 7(10) (2022) 901-904.
[92] K.N. Çerçi, I.R.O. Silva, K. Hooman, Investigation of the energetic and exergetic performance of hybrid rotary desiccant-vapor compression cooling systems using different refrigerants, Energy, (2024) 131732.
[93] J.-H. Cheng, Z.-Y. Wang, X. Cao, X.-Y. Li, C.-L. Zhang, Achieving deep dehumidification through a heat pump-boosted desiccant wheel system, Energy Conversion and Management, 313 (2024) 118604.

[94] M. Bozorgi, K. Ghasemi, S.H. Tasnim, S. Mahmud, Investigation of thermal comfort conditions by heat pump Hybridized with phase change Material-based solar desiccant cooling system, Applied Thermal Engineering, 232 (2023) 121097.
[95] S. Tian, X. Su, Y. Geng, H. Li, Y. Liang, Y. Di, Heat pump combined with single-stage or two-stage desiccant wheel system? A comparative study on different humidity requirement buildings, Energy Conversion and Management, 255 (2022) 115345.
[96] S. Tian, X. Su, H. Li, Y. Huang, Using a coupled heat pump desiccant wheel system to improve indoor humidity environment of nZEB in Shanghai: Analysis and optimization, Building and Environment, 206 (2021) 108391.
[97] F. Ge, C. Wang, Exergy analysis of dehumidification systems: A comparison between the condensing dehumidification and the desiccant wheel dehumidification, Energy conversion and management, 224 (2020) 113343.
[98] C. Naranjo-Mendoza, M.A. Oyinlola, A.J. Wright, R.M. Greenough, Experimental study of a domestic solar-assisted ground source heat pump with seasonal underground thermal energy storage through shallow boreholes, Applied Thermal Engineering, 162 (2019) 114218.
[99] S. Rayegan, S. Motaghian, G. Heidarinejad, H. Pasdarshahri, P. Ahmadi, M.A. Rosen, Dynamic simulation and multi-objective optimization of a solar-assisted desiccant cooling system integrated with ground source renewable energy, Applied Thermal Engineering, 173 (2020) 115210.
[100] J.-D. Liang, C.-L. Kao, L.-K. Tsai, Y.-C. Chiang, H.-C. Tsai, S.-L. Chen, Performance investigation of a hybrid ground-assisted desiccant cooling system, Energy Conversion and Management, 265 (2022) 115765.
[101] U. Berardi, G. Heidarinejad, S. Rayegan, H. Pasdarshahri, Enhancing the cooling potential of a solar-assisted desiccant cooling system by ground source free cooling, in: Building Simulation, Springer, 2020, pp. 1125-1144.
[102] G. Heidarinejad, U. Berardi, S. Rayegan, Performance investigation of ground source heat exchanger with desiccant-based hybrid cooling system in humid climate, in: IOP Conference Series: Materials Science and Engineering, IOP Publishing, 2019, pp. 052002.
[103] H. Ren, Z. Ma, W. Lin, W. Fan, W. Li, Integrating photovoltaic thermal collectors and thermal energy storage systems using phase change materials with rotary desiccant cooling systems, Sustainable cities and society, 36 (2018) 131-143.
[104] A. Kabeel, M. Abdelgaied, Solar energy assisted desiccant air conditioning system with PCM as a thermal storage medium, Renewable Energy, 122 (2018) 632-642.

[105] J. Song, B. Sobhani, Energy and exergy performance of an integrated desiccant cooling system with photovoltaic/thermal using phase change material and maisotsenko cooler, Journal of Energy Storage, 32 (2020) 101698.
[106] Z. Ma, H. Ren, Z. Sun, Energy and exergy analysis of a desiccant cooling system integrated with thermal energy storage and photovoltaic/thermal-solar air collectors, Science and Technology for the Built Environment, 26(1) (2020) 12-27.
[107] H. Yamauchi, A. Kodama, T. Hirose, H. Okano, K.-i. Yamada, Performance of VOC abatement by thermal swing honeycomb rotor adsorbers, Industrial & Engineering Chemistry Research, 46(12) (2007) 4316-4322.
[108] C.-M. Wang, T.-W. Chung, C.-M. Huang, H. Wu, Adsorption equilibria of acetate compounds on activated carbon, silica gel, and 13X zeolite, Journal of Chemical & Engineering Data, 50(3) (2005) 811-816.
[109] L. Zhu, D. Shen, K.H. Luo, A critical review on VOCs adsorption by different porous materials: Species, mechanisms and modification methods, Journal of hazardous materials, 389 (2020) 122102.
[110] T.N. Tu, T.M. Pham, Q.H. Nguyen, N.T. Tran, V.N. Le, L.H. Ngo, K. Chang, J. Kim, Metal–organic frameworks for aromatic-based VOC capture, Separation and Purification Technology, 333 (2024) 125883.
[111] C. Lai, Z. Wang, L. Qin, Y. Fu, B. Li, M. Zhang, S. Liu, L. Li, H. Yi, X. Liu, X. Zhou, N. An, Z. An, X. Shi, C. Feng, Metal-organic frameworks as burgeoning materials for the capture and sensing of indoor VOCs and radon gases, Coordination Chemistry Reviews, 427 (2021) 213565.
[112] Y. Sheng, L. Zhang, Y. Wang, L. Fang, Explore energy saving operation strategy: Indoor VOCs removal performance of silica gel rotor in clean-air heat pump system at low regeneration air temperature, Energy and Buildings, 202 (2019) 109379.
[113] Y. Sheng, L. Fang, Experimental analysis of the effect of moisture on air cleaning performance of desiccant wheel in a Clean Air Heat Pump, Building and Environment, 147 (2019) 551-558.
[114] Y. Sheng, L. Fang, Y. Sun, An experimental evaluation on air purification performance of Clean-Air Heat Pump (CAHP) air cleaner, Building and Environment, 127 (2018) 69-76.
[115] T. Ge, D. Qi, Y. Dai, R. Wang, Experimental testing on contaminant and moisture removal performance of silica gel desiccant wheel, Energy and Buildings, 176 (2018) 71-77.
[116] E.J. Wolfrum, D. Peterson, E. Kozubal, The Volatile Organic Compound (VOC) Removal Performance of Desiccant-Based Dehumidification Systems: Testing at Sub-ppm VOC Concentrations, HVAC&R Research, 14(1) (2008) 129-140.
[117] L. Fang, G. Zhang, A. Wisthaler, Desiccant wheels as gas-phase absorption (GPA) air cleaners: evaluation by PTR-MS and sensory assessment, Indoor Air, 18(5) (2008).

[118] S. Wang, L. Zhang, C. Long, A. Li, Enhanced adsorption and desorption of VOCs vapor on novel micro-mesoporous polymeric adsorbents, Journal of Colloid and Interface Science, 428 (2014) 185-190.
[119] E. Pérez-Botella, S. Valencia, F. Rey, Zeolites in adsorption processes: State of the art and future prospects, Chemical Reviews, 122(24) (2022) 17647-17695.
[120] T.S. Ge, D. Qi, Y.J. Dai, R.Z. Wang, Experimental testing on contaminant and moisture removal performance of silica gel desiccant wheel, Energy and Buildings, 176 (2018) 71-77.
[121] M. Fasihi, O. Efimova, C. Breyer, Techno-economic assessment of CO2 direct air capture plants, Journal of Cleaner Production, 224 (2019) 957-980.
[122] The Paris Agreement. https://unfccc.int/process-and-meetings/the-paris-agreement (accessed 02/13/2025).
[123] J. Liu, P.K. Thallapally, B.P. McGrail, D.R. Brown, J. Liu, Progress in adsorption-based CO2 capture by metal–organic frameworks, Chemical Society Reviews, 41(6) (2012) 2308-2322.
[124] F. Raganati, F. Miccio, P. Ammendola, Adsorption of Carbon Dioxide for Post-combustion Capture: A Review, Energy & Fuels, 35(16) (2021) 12845-12868.
[125] H. Zentou, M. Aliyu, M.A. Abdalla, O.Y. Abdelaziz, B. Hoque, A.M. Alloush, I.M. Tayeb, K. Patchigolla, M.M. Abdelnaby, Advancements and Challenges in Adsorption-Based Carbon Capture Technology: From Fundamentals to Deployment, The Chemical Record, 25(1) (2025) e202400188.
[126] F.N. Ridha, V. Manovic, A. Macchi, E.J. Anthony, CO2 capture at ambient temperature in a fixed bed with CaO-based sorbents, Applied Energy, 140 (2015) 297-303.
[127] I. Luz, M. Soukri, M. Lail, Flying MOFs: polyamine-containing fluidized MOF/SiO 2 hybrid materials for CO 2 capture from post-combustion flue gas, Chemical Science, 9(20) (2018) 4589-4599.
[128] J. Wu, K. Wang, J. Zhao, Y. Chen, Z. Gan, X. Zhu, R. Wang, C.-H. Wang, Y.W. Tong, T. Ge, A direct air capture rotary adsorber for CO2 enrichment in greenhouses, Device, (2024).
[129] T. Gupta, R. Ghosh, Rotating bed adsorber system for carbon dioxide capture from flue gas, International Journal of Greenhouse Gas Control, 32 (2015) 172-188.
[130] L. Herraiz, E. Palfi, E. Sánchez Fernández, M. Lucquiaud, Rotary adsorption: Selective recycling of CO2 in combined cycle gas turbine power plants, Frontiers in Energy Research, 8 (2020) 482708.
[131] J. Gao, Y. Hoshino, G. Inoue, Honeycomb-carbon-fiber-supported amine-containing nanogel particles for CO2 capture using a rotating column TVSA, Chemical Engineering Journal, 383 (2020) 123123.
[132] P. Eisenberger, Rotating multi-monolith bed movement system for removing CO2 from the atmosphere, in, Google Patents, 2018.
[133] Carbon Capture Technology. https://www.svanteinc.com/ (accessed 02/13/2025).
[134] Rotary Adsorption Machine. https://www.ljungstrom.com/ (accessed 02/13/2025).

[135] J. Liu, Y. Wang, A.I. Benin, P. Jakubczak, R.R. Willis, M.D. LeVan, CO2/H2O Adsorption Equilibrium and Rates on Metal−Organic Frameworks: HKUST-1 and Ni/DOBDC, Langmuir, 26(17) (2010) 14301-14307.
[136] J. Liu, A.I. Benin, A.M.B. Furtado, P. Jakubczak, R.R. Willis, M.D. LeVan, Stability Effects on CO2 Adsorption for the DOBDC Series of Metal–Organic Frameworks, Langmuir, 27(18) (2011) 11451-11456.
[137] P. Ilani-Kashkouli, J. Brechtl, K. An, M. Kidder, C. Tsouris, C. Janke, S. Kowalski, C.-M. Yang, M. Muneeshwaran, M. Lamm, K. Copenhaver, B. Fricke, X. Sun, K. Li, K. Nawaz, Demonstration of the carbon capture with building make-up air unit, Energy and Buildings, 325 (2024) 114966.
[138] K. An, J. Brechtl, S. Kowalski, C.-M. Yang, M.K. Kidder, C. Tsouris, C. Janke, M. Lamm, K. Copenhaver, J. Thompson, T. Turnaoglu, B. Fricke, K. Li, X. Sun, K. Nawaz, A multifunctional rooftop unit for direct air capture, Environmental Science: Advances, 3(6) (2024) 937-949.
[139] K. An, K. Li, C.-M. Yang, J. Brechtl, K. Nawaz, A comprehensive review on regeneration strategies for direct air capture, Journal of CO2 Utilization, 76 (2023) 102587.
[140] M. Sendi, M. Bui, N. Mac Dowell, P. Fennell, Geospatial analysis of regional climate impacts to accelerate cost-efficient direct air capture deployment, One Earth, 5(10) (2022) 1153-1164.
[141] H. Zhao, Q. Li, Z. Wang, T. Wu, M. Zhang, Synthesis of MIL-101 (Cr) and its water adsorption performance, Microporous and Mesoporous Materials, 297 (2020) 110044.
[142] S. Kayal, A. Chakraborty, H.W.B. Teo, Green synthesis and characterization of aluminium fumarate metal-organic framework for heat transformation applications, Materials Letters, 221 (2018) 165-167.
[143] T. Yang, L. Ge, T. Ge, G. Zhan, R. Wang, Binder‐free growth of aluminum‐based metal–organic frameworks on aluminum substrate for enhanced water adsorption capacity, Advanced Functional Materials, 32(5) (2022) 2105267.
[144] C. Petit, J. Burress, T.J. Bandosz, The synthesis and characterization of copper-based metal–organic framework/graphite oxide composites, Carbon, 49(2) (2011) 563-572.
[145] C. Petit, T.J. Bandosz, MOF–graphite oxide composites: combining the uniqueness of graphene layers and metal–organic frameworks, Advanced Materials, 21(46) (2009) 4753-4757.
[146] M. Jahan, Q. Bao, J.-X. Yang, K.P. Loh, Structure-directing role of graphene in the synthesis of metal− organic framework nanowire, Journal of the American Chemical Society, 132(41) (2010) 14487-14495.
[147] L. Li, X.L. Liu, H.Y. Geng, B. Hu, G.W. Song, Z.S. Xu, A MOF/graphite oxide hybrid (MOF: HKUST-1) material for the adsorption of methylene blue from aqueous solution, Journal of Materials Chemistry A, 1(35) (2013) 10292-10299.

[148] J. Yan, Y. Yu, C. Ma, J. Xiao, Q. Xia, Y. Li, Z. Li, Adsorption isotherms and kinetics of water vapor on novel adsorbents MIL-101 (Cr)@ GO with super-high capacity, Applied Thermal Engineering, 84 (2015) 118-125.
[149] K. Prasanth, P. Rallapalli, M.C. Raj, H. Bajaj, R.V. Jasra, Enhanced hydrogen sorption in single walled carbon nanotube incorporated MIL-101 composite metal–organic framework, International Journal of Hydrogen Energy, 36(13) (2011) 7594-7601.
[150] P. Somayajulu Rallapalli, M.C. Raj, D.V. Patil, K. Prasanth, R.S. Somani, H.C. Bajaj, Activated carbon@ MIL‐101 (Cr): a potential metal‐organic framework composite material for hydrogen storage, International Journal of Energy Research, 37(7) (2013) 746-753.
[151] B. Han, A. Chakraborty, Water adsorption studies on synthesized alkali-ions doped Al-fumarate MOFs and Al-fumarate+ zeolite composites for higher water uptakes and faster kinetics, Microporous and Mesoporous Materials, 288 (2019) 109590.
[152] Z. Liu, C. Cheng, J. Han, X. Qi, Z. Zhao, R. Teng, Dehumidification performance of aluminum fumarate metal organic framework and its composite, Applied Thermal Engineering, 199 (2021) 117570.
[153] T.M. McDonald, J.A. Mason, X. Kong, E.D. Bloch, D. Gygi, A. Dani, V. Crocella, F. Giordanino, S.O. Odoh, W.S. Drisdell, Cooperative insertion of CO2 in diamine-appended metal-organic frameworks, Nature, 519(7543) (2015) 303-308.
[154] B. Han, A. Chakraborty, Functionalization, protonation and ligand extension on MIL-53 (Al) MOFs to boost water adsorption and thermal energy storage for heat transformations, Chemical Engineering Journal, 472 (2023) 145137.
[155] J.A. Shamim, S. Paul, K. Kitaoka, W.-L. Hsu, H. Daiguji, Experimental evaluation of transient heat and mass transfer during regeneration in multilayer fixed-bed binder-free desiccant dehumidifier, International Journal of Heat and Mass Transfer, 128 (2019) 623-633.
[156] K. Ebrahimi, G.F. Jones, A.S. Fleischer, A review of data center cooling technology, operating conditions and the corresponding low-grade waste heat recovery opportunities, Renewable and Sustainable Energy Reviews, 31 (2014) 622-638.
[157] X. Chen, X. Wang, T. Ding, Z. Li, Experimental research and energy saving analysis of an integrated data center cooling and waste heat recovery system, Applied Energy, 352 (2023) 121875.
[158] G. Goodarzia, N. Thirukonda, S. Heidari, A. Akbarzadeh, A. Date, Performance evaluation of solid desiccant wheel regenerated by waste heat or renewable energy, Energy Procedia, 110 (2017) 434-439.
[159] Y. Zhang, X. He, Z. Zhu, W.-N. Wang, S.-C. Chen, Simultaneous removal of VOCs and PM2. 5 by metal-organic framework coated electret filter media, Journal of Membrane Science, 618 (2021) 118629.